Patterns in rectangulations. Part I: ⊤-like patterns, inversion sequence classes $I(010, 101, 120, 201)$ and $I(011, 201)$, and rushed Dyck paths

Andrei Asinowski[1*]   Michaela A. Polley[1,2†]

[1] *University of Klagenfurt, Klagenfurt, Austria*
[2] *Dartmouth College, Hanover, NH, USA*

We initiate a systematic study of *pattern avoidance in rectangulations*. We give a formal definition of such patterns and investigate rectangulations that avoid ⊤-like patterns — the pattern ⊤ and its rotations. For every $L \subseteq \{⊤, ⊣, ⊥, ⊢\}$ we enumerate L-avoiding rectangulations, both weak and strong. In particular, we show ⊤-avoiding *weak* rectangulations are enumerated by Catalan numbers and construct bijections to several Catalan structures. Then, we prove that ⊤-avoiding *strong* rectangulations are in bijection with several classes of inversion sequences, among them $I(010, 101, 120, 201)$ and $I(011, 201)$ — which leads to a solution of the conjecture that these classes are Wilf-equivalent. Finally, we show that $\{⊤, ⊥\}$-avoiding strong rectangulations are in bijection with recently introduced rushed Dyck paths.

Keywords: Rectangulations, inversion sequences, Dyck paths, pattern avoidance

1   Introduction

A rectangulation $\mathcal{R}$ is a decomposition of a rectangle R into a finite number of rectangles. Rectangulations appear naturally in integrated circuit design [25, 27], combinatorial and geometric algorithms [16, 21, 38, 47], scientific data visualization [8, 24], architecture [17, 33, 40], and also in visual art and design. They are of interest to combinatorialists due to their rich structure and many links to other combinatorial objects. For example, classes of rectangulations have been shown to be in bijection with permutation classes, binary trees, posets, Hopf algebras, planar maps, among others [1, 4, 14, 15, 26, 30, 31, 37].

arXiv:2501.11781v4 [math.CO] 6 Oct 2025

Our work concerns pattern avoidance in rectangulations. Rectangulation patterns were considered, explicitly or implicitly, in several earlier contributions in the areas of combinatorics, computational geometry, and geometric algorithms. A rectangulation is *guillotine* if and only if it avoids both *windmills* � and ⊥: this early result was mentioned in many papers on algorithmic floorplaning; to our knowledge, the first combinatorial paper where it appeared is [1] by Ackerman, Barequet, and Pinter. Cardinal, Sacristán, and Silveira [10] showed that a rectangulation is (strongly equivalent to) a diagonal one if and only if it avoids the patterns ⊥ and ⊤. Generating functions for some families of pattern-avoiding rectangulations were found by Asinowski and Mansour [5]. Eppstein, Mumford, Speckmann, and Verbeek [13] proved that a rectangulation is *area-universal* is and only if every one of its segment is *one-sided*: from the perspective of patterns, these are precisely $\{\vdash, \dashv, \top, \bot\}$-avoiding rectangulations. More recently, pattern avoidance in rectangulations was considered by Merino and Mütze [32] in the context of algorithmic generation of combinatorial structures, where eight specific patterns were considered for demonstrating the developed algorithm. Asinowski and Banderier [3] provided an analytic solution for several models involving these patterns — in particular, all models from [32] that deal with weak guillotine rectangulations. Finally, Asinowski, Cardinal, Felsner, and Fusy [4] proved several results about correspondence of rectangulation patterns to permutation patterns — in particular a characterization (conjectured by Merino and Mütze) of strong guillotine rectangulations by *mesh patterns*.

Our goal is to initiate a systematic treatment of this topic; therefore, we start this contribution with giving a precise definition of pattern avoidance in rectangulations. Then we explore the case of ⊤-like patterns — that is, the patterns ⊤, ⊢, ⊥, and ⊣. For every possible subset L of these patterns, we enumerate rectangulations that avoid L, and we provide bijections with classes of structures, such as inversion sequences, permutations, and Dyck paths. Our main results include bijections between ⊤-avoiding strong rectangulations and several classes of inversion sequences, among them $I(010, 101, 120, 201)$ and $I(011, 201)$. At the time of writing, the former of these classes is *known* to be enumerated by the sequence A279555 of the OEIS [35], and the latter is *conjectured* to be enumerated by the same sequence [9, 48]. Our results include a proof of this conjecture, and, at the same time, offer the first combinatorial interpretation of A279555 other than as a class of inversion sequences. Our further results include a bijection between $\{\top, \bot\}$-avoiding strong rectangulations and a recently introduced family of rushed Dyck paths, enumerated by A287709. In summary, already the simplest cases of pattern avoidance in rectangulations lead to interesting results and connections.

In the follow-up articles we study representation of rectangulation patterns by permutation patterns, and explore the cases where avoided patterns consist of three segments. The ultimate goal of our study is to develop general approaches, similar to the areas of pattern avoidance in permutations, posets, lattice paths, etc. For instance, given a set of patterns L, we wish to know whether L-avoiding rectangulations are bijective to a class of permutations or inversion sequences, and whether the generating function is rational / algebraic / D-finite or not. In earlier contributions such questions were handled ad hoc, we wish to develop a systematic approach.

The motivation behind investigating the ⊤-like patterns is two-fold. These are the simplest patterns, and it is very natural to start the systematic study with exploring them in order to see which phenomena can be observed when they determine a class of rectangulations (for instance, the difference between the "weak" and the "strong" case). On the other hand, since all the joints in generic rectangulations have a ⊤ shape, any pattern can be regarded as composed of several ⊤-like patterns. Hence, good understanding of their avoidance is an essential step towards a general theory.

The paper is organized as follows: In Section 2 we provide the background and recall main definitions and basic results on rectangulations and inversion sequences. In Section 3 we give a precise definition of patterns in rectangulations. Then we present our results, in particular: in Section 4.1.1 we provide bijections between ⊤-avoiding weak rectangulations and several Catalan structures (Theorem 1); in Sections 4.1.3 and 4.1.4, bijections between ⊤-avoiding strong rectangulations and avoidance classes of inversion sequences, including $I(010, 101, 120, 201)$ and $I(011, 201)$ (Theorems 4 and 6); and, in Section 4.2.2, bijections between $\{⊤, ⊥\}$-avoiding strong rectangulations and rushed Dyck paths (Theorem 13).

2   Definitions and basics

2.1   Rectangulations

In this expository section we recall definitions and basic results on rectangulations. All the results are taken from [1, 2, 4, 10, 32]. In most cases we follow the conventions and the notation from [4].

Rectangulations and segments.   A rectangulation $\mathcal{R}$ of an axis-aligned rectangle R is a decomposition of R into finitely many interior-disjoint rectangles. The *size* of $\mathcal{R}$ is the number of rectangles in the decomposition. See Figure 1 for several rectangulations of size 9.

A *segment* in $\mathcal{R}$ is a union of one or more sides of rectangles that form a straight line, is maximal in regards to this property, and is not one of the sides of R. We will always assume that the rectangulations are *generic*, which means that segments do not cross each other; that is, two segments can meet in a joint of the shape ⊤, ⊥, ⊢, or ⊣, but never +. Under this assumption, every rectangulation of size n has precisely $n-1$ segments. Given a segment s, a *neighboring segment* of s is a perpendicular segment one of whose endpoints lies on s, and a *neighboring rectangle* of s is a rectangle of $\mathcal{R}$ one of whose sides is included in s. Depending on the side from which a neighboring segment (or rectangle) meets s, we call it a left, right, top, or bottom neighboring segment (or rectangle). A segment is one-sided if it has neighboring segments on at most one of its sides.
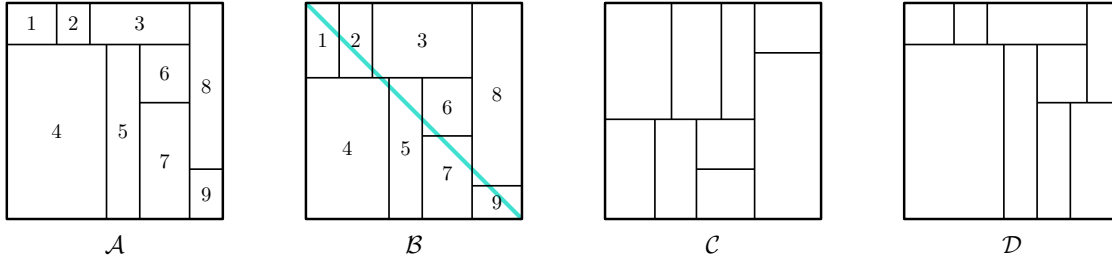

Fig. 1: Four rectangulations of size 9. Rectangulations $\mathcal{A}$, $\mathcal{B}$, and $\mathcal{C}$ are weakly equivalent. Rectangulations $\mathcal{A}$ and $\mathcal{B}$ are also strongly equivalent. Rectangulation $\mathcal{B}$ is diagonal. For rectangulations $\mathcal{A}$ and $\mathcal{B}$, the NW–SE labeling is shown.

Weak and strong equivalence   There are two natural ways to define equivalence classes for rectangulations: the *weak equivalence* that preserves segment-to-rectangle contacts, and the (finer) *strong equivalence* that preserves rectangle-to-rectangle contacts.

A precise definition is based on *neighborhood relations* between rectangles of $\mathcal{R}$. A rectangle Y is *right* of a rectangle X (equivalently, X is *left* of Y) if there exists a sequence of rectangles $X = X_1, X_2, \ldots, X_k = Y$ such that for every i, $1 \leq i \leq k - 1$, there is a vertical segment s_i such that X_i is a left neighbor of s_i and X_{i+1} is a right neighbor of s_i. A rectangle Y is *above* a rectangle X (equivalently, X is *below* Y) if there exists a sequence of rectangles $X = X_1, X_2, \ldots, X_k = Y$ such that for every i, $1 \leq i \leq k - 1$, there is a horizontal segment s_i such that X_i is a bottom neighbor of s_i and X_{i+1} is a top neighbor of s_i. Every pair X, Y of distinct rectangles of $\mathcal{R}$ satisfies precisely one of these relations: X is either above, below, right of, or left of Y.

Two rectangulations are *weakly equivalent* if there is a (unique) bijection between their rectangles that preserves the left–right and above–below neighborhood relations. Two rectangulations are *strongly equivalent* if this bijection additionally preserves contacts between rectangles. Every weak rectangulation produces one or several strong rectangulations which differ from each other by *shufflings* — the orders in which each segment meets the endpoints of all neighboring segments.

A *weak rectangulation* is an equivalence class of rectangulations with respect to the weak equivalence, and a *strong rectangulation* is an equivalence class of rectangulations with respect to the strong equivalence. In Figure 1, the rectangulations $\mathcal{A}$, $\mathcal{B}$, and $\mathcal{C}$ are weakly equivalent, but only $\mathcal{A}$ and $\mathcal{B}$ are strongly equivalent. Hence, the four images in Figure 1 represent two distinct weak rectangulations but three distinct strong rectangulations.

Diagonal labelings   We denote the sides of R by the cardinal directions N (top), W (left), S (bottom), and E (right), and, accordingly, the corners by NW, SW, SE, and NE. A *W-rectangle* is any rectangle that touches W, the *NW-rectangle* is the rectangle that contains the NW-corner, and similar for other sides and corners. The *NW–SE ordering* of the rectangles of $\mathcal{R}$ is the order in which $X \prec Y$ if and only if X is left of or above Y. The *NW–SE labeling* is the labeling of the rectangles by $1, 2, 3, \ldots, n$ according to the NW–SE ordering, see rectangulations $\mathcal{A}$ and $\mathcal{B}$ in Figure 1. In the NW–SE labeling, rectangle Y is the direct successor of rectangle X if and only if there is a segment whose one endpoint is the SE-corner of X and the other endpoint is the NW-corner of Y. One similarly defines SW–NE, SE–NW, and NE–SW orderings and labelings.

Diagonal rectangulations   A *diagonal rectangulation* is a rectangulation in which the NW–SE diagonal of R intersects the interior of every rectangle. In Figure 1, $\mathcal{B}$ is a diagonal rectangulation. Every rectangulation $\mathcal{R}$ is weakly equivalent to a diagonal rectangulation. Moreover, all diagonal rectangulations weakly equivalent to $\mathcal{R}$ lie in the same strong equivalence class, in which all the segments are shuffled so that the configurations ⊣ and ⊤ are avoided. In a diagonal rectangulation, the NW–SE diagonal intersects the rectangles according to the NW–SE ordering.

Guillotine rectangulations   A *cut* in $\mathcal{R}$ is a segment whose endpoints lie on opposite sides of R. A rectangulation $\mathcal{R}$ is *guillotine* if it is either of size 1, or contains a cut that splits it into two sub-rectangulations which are (recursively) both guillotine. In Figure 1, the rectangulations $\mathcal{A}, \mathcal{B}, \mathcal{C}$ are guillotine, and $\mathcal{D}$ is non-guillotine. A rectangulation is guillotine if and only if it avoids *windmills* — quadruples of segments of the shape ⊞ or ⊟.

2.2   Inversion sequences

In this section we recall the basic definitions related to inversion sequences and pattern avoidance in them.

An *inversion sequence* of length n is an integer sequence $e = (e_1, e_2, e_3, \ldots, e_n)$ such that $0 \leq e_j \leq$

$j - 1$ holds for all $j \in [n]$. We denote the set of all inversion sequences of length n by I_n. An inversion sequence of length n can be plotted on the lower staircase of a $n \times n$ grid by labeling the columns from 1 to n and the rows from 0 to $n - 1$, see Figure 2 for an example.
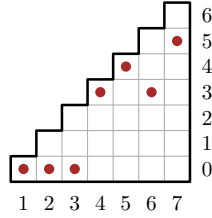

Fig. 2: Plot of the inversion sequence $e = (0, 0, 0, 3, 4, 3, 5)$.

Given an inversion sequence e, we say that e_j is *high* if $e_j = j - 1$. Further, the *bounce*[i] of e is $k := n - M$, where n is the length of e, and M is its maximum value. The inversion sequence $e = (0, 0, 0, 3, 4, 3, 5)$ from Figure 2 has three high elements, three 0 elements, and its bounce is 2. Its left-to-right maxima are $0, 3, 4, 5$, and its right-to-left minima are $0, 3, 5$.

There is a natural size-preserving bijection Θ from permutations to inversion sequences: A permutation $\pi = \pi_1 \pi_2 \ldots \pi_n \in S_n$ is mapped to the inversion sequence $e = (e_1, e_2, e_3, \ldots, e_n) \in I_n$, where e_k is the number of inversions whose second (smaller) element is π_k, that is, $e_k = |\{i : 1 \leq i < k, \pi_i > \pi_k\}|$. In this case we say that e is the inversion sequence of π. For example, $(0, 0, 0, 3, 4, 3, 5) \in I_7$ is the inversion sequence of $5673142 \in S_7$.

Similar to pattern avoidance in permutations (refer to [7] for main definitions and basic results), one defines pattern avoidance in inversion sequences, with the caveat that a pattern is not necessarily a valid inversion sequence itself, but can be any sequence f of non-negative integers with set of values $\{0, 1, 2, \ldots, \ell\}$ for some ℓ. For example, $(1, 0)$ is not an inversion sequence, but it can be considered as a pattern. An inversion sequence e *contains* f if e has a (not necessarily contiguous) subsequence whose entries have the same relative order as f. Otherwise, e *avoids* f. All the patterns in our paper are of the length at most 3, and we write them without parentheses and commas, for example 201 rather then $(2, 0, 1)$. For example, the inversion sequence from Figure 2 contains — among others — the patterns 001, 010, 021, 102, but avoids the patterns 100, 101, 120, 210. Given a set of patterns T, an inversion sequence is T-*avoiding* if it avoids all the patterns from T. We denote the set of T-avoiding inversion sequences by $I(T)$, and the set of T-avoiding inversion sequences of length n by $I_n(T)$. For two sets of patterns, T and T', we say that the classes $I(T)$ and $I(T')$ are *Wilf-equivalent* if $|I_n(T)| = |I_n(T')|$ for every $n \geq 1$; we denote this by $I(T) \sim I(T')$. A systematic investigation of pattern avoidance in inversion sequences was started in [12, 28, 29], and it is still a very active area of research.

3 Pattern avoidance in rectangulations

As mentioned above, we aim to developing a systematic study of patterns in rectangulations. Therefore, in this section we give a formal definition of rectangulation patterns in terms of configurations of segments.

---

[i] This term was coined by Jay Pantone in [36].

Definition. A *configuration of segments* is a connected[(ii)] set of horizontal and vertical segments such that two distinct segments never cross and never share an endpoint. Two configurations of segments, C and C', are *weakly equivalent* if there is a (unique) bijection $\gamma \colon s \mapsto s'$ between their segments such that

1. Segments $s \in C$ and $s' \in C'$ have the same orientation (both are horizontal or both are vertical);

2. Segments s and t meet in C if and only if segments s' and t' meet in C', and the respective joints are of the same kind;

3. For every segment s, the order in which its neighboring segments meet it is preserved by γ, independently, for both sides of s. (More precisely, if s is vertical, and $t_1, t_2, \ldots, t_k$ are its left neighboring segments listed in the order in which s meets them from the top to the bottom, then $t'_1, t'_2, \ldots, t'_k$ are precisely the left neighboring segments of s' listed in the order in which s' meets them from the top to the bottom; similarly for the right neighboring segments of s; and similarly for a horizontal s.)

Finally, C and C' are *strongly equivalent* if they are weakly equivalent and the bijection γ also satisfies

4. For every segment s, the order in which *all* the neighbors of s meet it, is preserved by γ. (More precisely, if s is vertical, and $t_1, t_2, \ldots, t_k$ are precisely the neighboring segments of s listed in the order in which s meets them from the top to the bottom, then $t'_1, t'_2, \ldots, t'_k$ are precisely the neighboring segments of s' listed in the order in which s' meets them from the top to the bottom; similarly for a horizontal s.)

Definition. A *weak rectangulation pattern* is an equivalence class of configurations of segments with respect to the weak equivalence. A *strong rectangulation pattern* is an equivalence class of configuration of segments with respect to the strong equivalence.

A rectangulation $\mathcal{R}$ *contains* a pattern p if there is an injection from the segments of (any representative of) p into the segments of (any representative of) $\mathcal{R}$ which preserves incidences, orientations, and order of incidence of neighbors of the segments of p. Otherwise, $\mathcal{R}$ *avoids* p.

Here, the order of incidence should be understood according to the kind of equivalence. For weak rectangulations we consider weak patterns, and for strong rectangulations we consider strong patterns[(iii)].

The next figures illustrate these concepts and present some phenomena. In Figure 3, all three segment configurations are weakly equivalent, but only (a) and (b) are strongly equivalent. Accordingly, (a) and (b) represent the same strong pattern, and (c) a different strong pattern; but all three configurations represent the same weak pattern. The colors are used in order to make the correspondence visually clear.

Since patterns involve only segments, there is a greater flexibility in drawing their representatives than for rectangulations. For example, images (a) and (b) in Figure 4 represent the same pattern. (In this case, all the segments are one-sided, therefore this pattern can be seen as a weak or as a strong pattern.) Moreover, an occurrence of a pattern p in a rectangulation preserves all the contacts that exist in p, but can also contain some additional contacts: this is also illustrated in Figure 4(c).

Let L be a set of rectangulation patterns. Denote by $R^w(L)$ and $R^s(L)$ the set of weak and, respectively, strong rectangulations that avoid all the patterns from L. We refer to these sets as *rectangulation classes*.

[(ii)] Considering disconnected patterns would inevitably involve configurations of both segments and rectangles and lead to more involved definitions. Yet in [3, 32] some disconnected patterns were considered, rather *ad hoc*.

[(iii)] Avoidance of strong patterns in weak rectangulations is in general not well defined, and avoidance of weak patterns in strong rectangulations is equivalent to avoidance of several strong patterns.
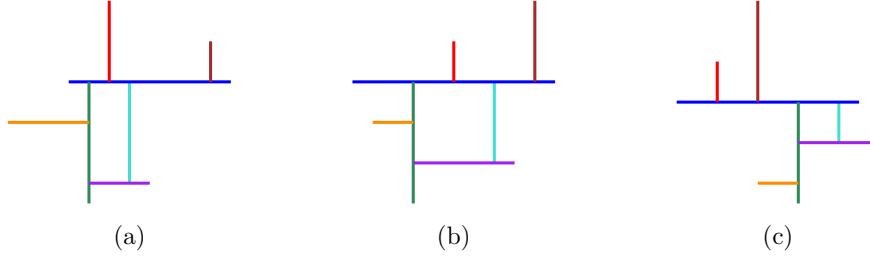
Fig. 3: Images (a) and (b) represent the same strong pattern, and (c) a different strong pattern. All three images represent the same weak pattern.
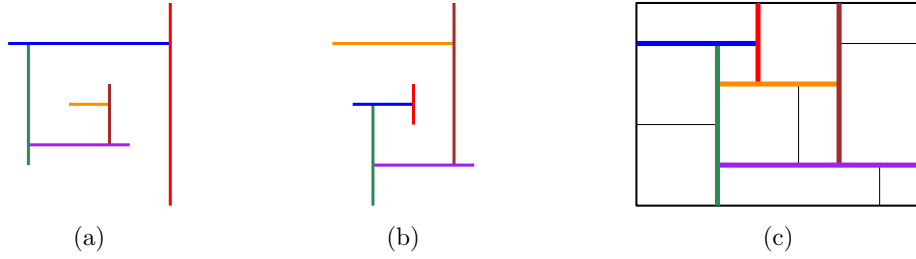

Fig. 4: Two drawings of the same pattern (a,b), and its occurrence in a rectangulation (c).

Note that if L contains at least one pattern from $\{\top, \bot\}$ and at least one pattern from $\{\vdash, \dashv\}$, then all the segments in the rectangulations of the class are one-sided, and hence, the distinction between $R^w(L)$ and $R^s(L)$ is not essential: in this case we simply write $R(L)$. To refer to L-avoiding rectangulations of a fixed size n, we add a subscript and denote the respective sets by $R_n^w(L)$, $R_n^s(L)$, and $R_n(L)$.

4 L-avoiding rectangulations for $L \subseteq \{\top, \vdash, \bot, \dashv\}$

In this section, we investigate the basic case of ⊤-*like patterns* — that is, the pattern ⊤ and its rotations $\dashv, \bot, \vdash$. A summary of our main enumerative results is given in Table 1. There are five essentially different combinations L of ⊤-like patterns. In Section 4.1 we explore ⊤-avoiding rectangulations, and in Section 4.2, $\{\top, \bot\}$−avoiding rectangulations. Only in these two cases is distinction between weak and strong rectangulations (indicated by **w** and **s** in the table) essential. The last three cases are elementary, we give them in Section 4.3.

4.1 *Enumeration and bijections for* $R(\top)$

We start with the most basic case: $L = \{\top\}$. Note that ⊤-avoiding rectangulations are precisely those in which every vertical segment reaches N. We explore ⊤-avoiding weak rectangulations in Section 4.1.1, and then ⊤-avoiding strong rectangulations in Sections 4.1.3–4.1.4. In Section 4.1.2 we provide a background on $I(010, 101, 120, 201)$ and $I(011, 201)$ (and some other related classes of inversion sequences), and in Section 4.1.5 we use our results to prove Wilf-equivalence of these two classes, along with several matching statistics.

L	**w/s**	Formula/OEIS	Bijection to...
$\{\top\}$	**w**	A000108 (Catalan numbers)	Binary trees, Dyck paths, (10)-avoiding inversion sequences, (213)-avoiding permutations
	s	A279555	$I(010,101,120,201)$, $I(010,110,120,210)$ $I(010,100,120,210)$, and $I(011,201)$.
$\{\top,\bot\}$	**w**	2^{n-1}	Compositions
	s	A287709	Rushed Dyck paths
$\{\top,\vdash\}$		2^{n-1}	Binary sequences
$\{\top,\vdash,\bot\}$		n	
$\{\top,\vdash,\bot,\dashv\}$		2	

Tab. 1: Summary of main results on enumeration of L-avoiding rectangulations for $L \subseteq \{\top,\vdash,\bot,\dashv\}$.

4.1.1 $\top$-*avoiding weak rectangulations: bijections with Catalan structures*

Enumeration of $R^w(\top)$ leads to a famous sequence:

Theorem 1. $|R_n^w(\top)| = C_n$, *the n-th Catalan number.*

This result, as well as its proof via binary trees (Proof 2 below), was first found by Aaron Williams [46]. We provide several proofs: first we derive the generating function for $R_n^w(\top)$, and then we construct bijections between $R_n^w(\top)$ and several standard Catalan structures, such as binary trees, Dyck paths, (213)-avoiding permutations, and (10)-avoiding inversion sequences. These proofs emphasize different aspects of the result: bijections to binary trees and Dyck paths demonstrate that $\top$-avoiding weak rectangulations is a very natural Catalan structure; the bijection with (213)-avoiding permutations shows how adding the pattern $\top$ restricts the well-known bijection between weak rectangulations and Baxter permutations; finally, the bijection τ with (10)-avoiding inversion sequences is used in Section 4.1.3 as a basis for bijections between $\top$-avoiding *strong* rectangulations and several classes of pattern-avoiding inversion sequences.

Proof 1: Generating functions. In this proof we consider a structural decomposition of $\top$-avoiding rectangulations, and translate it into an equation satisfied by the generating function. It is an adaptation of the proof of the claim that (all) weak rectangulations are enumerated by Schröder numbers (see [2, Theorem 2] and [4, Proposition 2.4]).

Let $\mathcal{R} \in R^w(\top)$. Note that $\mathcal{R}$ is necessarily guillotine, since both windmills contain $\top$. Every guillotine rectangulation of size > 1 has either horizontal or vertical cut(s) and is called accordingly horizontal or vertical. Let $R(x)$, $H(x)$, and $V(x)$ be the generating functions (with respect to the size) for all, horizontal, and vertical rectangulations in $R^w(\top)$, respectively. Then we have

$$R(x) = x + H(x) + V(x). \tag{1}$$

Consider the structural decomposition of horizontal and vertical rectangulations in $R^w(\top)$ (see Figure 5). Given a horizontal rectangulation in $R^w(\top)$, let s be its lowest cut. Above s there can be any
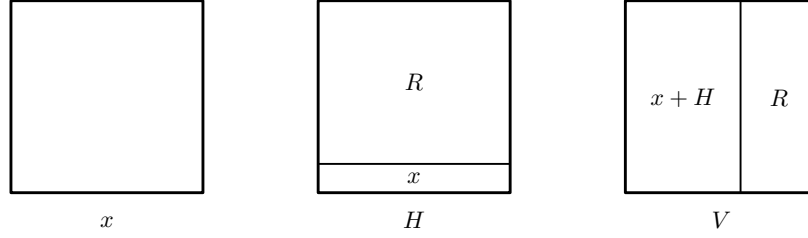
Fig. 5: The structural decomposition of an element of $R^w(\top)$.

⊤-avoiding rectangulation; below s there can be a only a single non-partitioned rectangle. Hence, we have

$$H(x) = x\,R(x). \tag{2}$$

Given a vertical rectangulation in $R^w(\top)$, let t be its left-most cut. To the left of t there can be either a rectangulation of size 1 or any ⊤-avoiding horizontal rectangulation; to the right of t there can be any ⊤-avoiding rectangulation. Hence, we have

$$V(x) = \big(x + H(x)\big)\,R(x). \tag{3}$$

Solving (1), (2), and (3) for $R(x)$, we obtain

$$xR^2(x) + (2x - 1)R(x) + x = 0,$$

which yields

$$R(x) = \frac{1 - \sqrt{1 - 4x}}{2x} - 1,$$

the generating function of Catalan numbers (starting at C_1). □

Proof 2: Bijection with binary trees and staircases. As mentioned above, this proof was first given by Aaron Williams [46]. It employs the fact that every diagonal rectangulation can be decomposed into two binary trees by cutting along the diagonal: see Figure 6(a), where the *lower tree* is red and the *upper tree* is blue. More precisely, there is a bijection between weak rectangulations and *twin-binary trees* — pairs of binary trees that satisfy a condition to match the orientations of interior leaves [49]. Below we show that ⊤-*avoiding* weak rectangulations are in bijection with *individual* binary trees.

Given a ⊤-avoiding weak rectangulation $\mathcal{R}$, consider its diagonal drawing. Since ⊤ is avoided, all the joints that lie above the diagonal are of the shape ⊣. Therefore, the upper binary tree — and hence, the entire rectangulation — is entirely determined by the lower binary tree. This leads to the bijection which maps $\mathcal{R}$ to the lower binary tree obtained in this way. For a binary tree $\mathcal{T}$, the corresponding ⊤-avoiding diagonal rectangulation can be constructed as follows (see Figure 6(b)):

1. Embed $\mathcal{T}$ in a rectangle R so that its root is in the SW-corner, all the edges are horizontal or vertical and non-crossing, and all the leaves lie on the NW–SE diagonal.

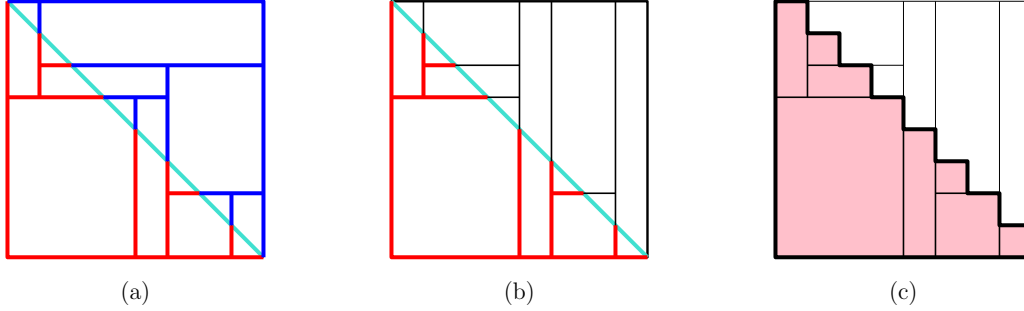2. Extend every vertical edge upwards until it meets N — the top side of R.

Fig. 6: Illustration to the second proof of Theorem 1. (a) A diagonal rectangulation is uniquely determined by a pair of binary trees. (b) A ⊤-avoiding diagonal rectangulation is uniquely determined by a single binary tree. (c) A ⊤-avoiding diagonal rectangulation is uniquely determined by a Catalan staircase (pink).

   3. Extend every horizontal branch rightwards until it meets a vertical segment or E — the right side of R.

Since binary trees are enumerated by Catalan numbers [39, Chapter 2, item 5], the result follows.

In fact, a minor modification of the subdiagonal part of ⊤-avoiding rectangulations recovers *Catalan staircases*. They are defined in [39, Chapter 2, item 205] as "tilings of the staircase shape [with n steps] by n rectangles", and they are clearly equivalent to binary trees: see Figure 6(c). □

Proof 3: Bijection with non-decreasing inversion sequences and Dyck paths. We establish a size-preserving bijection τ from ⊤-avoiding weak rectangulations to non-decreasing inversion sequences, which then directly yields a bijection with Dyck paths. Note that the family of non-decreasing inversion sequences is precisely $I(10)$. Every non-decreasing inversion sequence e consists of *plateaus* — maximal consecutive subsequences with the same value. The first elements of the plateaus are precisely the left-to-right maxima of e. Consecutive plateaus are separated by a *jump* — a pair of consecutive elements e_i, e_{i+1} with $e_i < e_{i+1}$; the *height* of such a jump is $e_{i+1} - e_i$.

Let $\mathcal{R} \in R^w(\top)$. We construct a non-decreasing inversion sequence $\tau(\mathcal{R})$ as follows:

   1. For each rectangle X of $\mathcal{R}$, label it with the number of rectangles to the left of X. This labeling will be called the *L-labeling*.

   2. Consider also the SW–NE ordering of the rectangles of $\mathcal{R}$.

   3. We define $\tau(\mathcal{R})$ to be the sequence e obtained by taking the rectangles according to the SW–NE ordering and reading their L-labels.

These steps are demonstrated in Figure 7(a,b,c). For the rectangulation $\mathcal{R}$ in this example we obtain $\tau(\mathcal{R}) = (0, 0, 1, 1, 1, 4, 4, 4, 4, 8, 8, 12, 12, 12, 12, 12, 12)$.

To see that e is an inversion sequence, note that if $Y_k \in \mathcal{R}$ is the rectangle labeled k in the SW–NE labeling, then there are *precisely* $k - 1$ rectangles which lie left of or below Y_k, and therefore, *at most* $k - 1$ rectangles left of Y_k: hence, $e_k \leq k - 1$. To see that e is non-decreasing, consider Y_k and Y_{k+1}, the rectangles of $\mathcal{R}$ labeled (respectively) k and $k + 1$ in the SW–NE labeling. Then Y_{k+1} is either to the
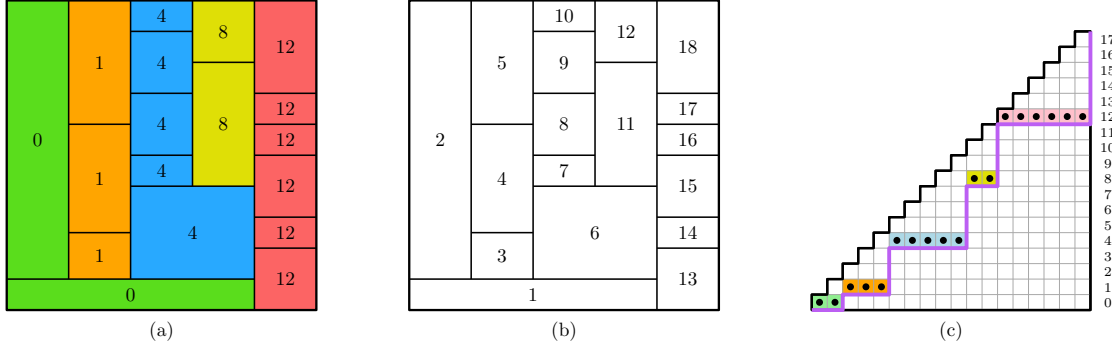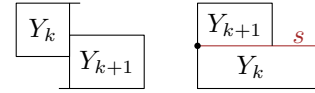
Fig. 7: Bijection $\tau\colon R^w(\top) \to I(10)$: (a) Rectangulation $\mathcal{R}$ with the L-labeling; (b) Rectangulation $\mathcal{R}$ with the SW–NE labeling; (c) The inversion sequence $e = \tau(\mathcal{R})$ and the Dyck path $p = \delta(\mathcal{R})$.

right of or above Y_k. In the former case the L-label of Y_k is clearly smaller than that of Y_{k+1}, which means $e_k < e_{k+1}$. In the latter case there is a horizontal segment s which contains the top side of Y_k and the bottom side of Y_{k+1}. The left endpoint of s is the SW-corner of Y_{k+1} and, since $\mathcal{R}$ avoids $\top$, it is also the NW-corner of Y_k. Hence, the set of rectangles left of Y_k and the set of rectangles left of Y_{k+1}

are the same. Therefore, in this case, the L-labels of Y_k and of Y_{k+1} are equal, and we have $e_k = e_{k+1}$.

The result $|I_n(10)| = C_n$ was shown in several contributions: see, for example, [29, Theorem 27] and [41, Section 2.1]. The following direct bijection ε from non-decreasing inversion sequences to Dyck paths is given in [39, Chapter 2, item 78]: Given $e \in I_n(10)$, consider its plot drawn over in the $[0,n] \times [0,n]$ grid. Connect the point $(0,0)$ to the point (n,n) by the lattice path which consists of $(1,0)$-steps just below the cells marked in the plot, and $(0,1)$-steps which are then needed to complete such a path. This lattice path is a (subdiagonal) Dyck path $\varepsilon(e)$ of semilength n, and it is clear that ε is bijective. Then $\delta := \varepsilon \circ \tau$ is a mapping from $R^w(\top)$ to Dyck paths of semilength n. In Figure 7(c), the Dyck path $p = \delta(\mathcal{R})$ is shown by a purple line.

We now make several observations that will be useful later. Denote the left side, the vertical segments, and the right side of $\mathcal{R}$, ordered from left to right, by $s_1, s_2, \ldots, s_{t+1}$. Two rectangles have the same L-label if and only if they are right neighbors of the same s_k. When we construct $\tau(\mathcal{R})$ by taking the rectangles of $\mathcal{R}$ according to the SW–NE ordering, we first take the right neighbors of s_1, then the right neighbors of s_2, and so on; for each $k = 1, 2, \ldots, t$, the right neighbors of s_k are taken from bottom to top. Therefore, the length of the k-th plateau is equal to the number of rectangles that neighbor s_k on the right. Finally, for $k \geq 2$, the set of rectangles to the left of s_k is the disjoint union of rectangles to the left of s_{k-1} and the left neighbors of s_k. Therefore, the height of the jump from the $(k-1)$-th to the k-th plateau is equal to the number of left neighbors of s_k.

As a result, the Dyck path $\delta(\mathcal{R})$ can be directly obtained as follows: Given $\mathcal{R} \in R^w(\top)$, we traverse it as shown by the white arrow in Figure 8(a): beginning in the SW-corner and ending in the SE-corner, we trace the left, right, and top sides of R (W, E, and N) and each of the vertical segments in $\mathcal{R}$. Each rectangle we cross as we trace upwards corresponds to a $(1,0)$-step in the Dyck path and each rectangle

we cross as we trace downwards corresponds to a $(0, 1)$-step in the Dyck path. If we use instead $(1, 1)$-and $(1, -1)$-steps, we directly obtain the standard form of p. Then, for every rectangle X of $\mathcal{R}$, the left and the right sides of X correspond to a matching pair of steps in p, see Figure 8(b).

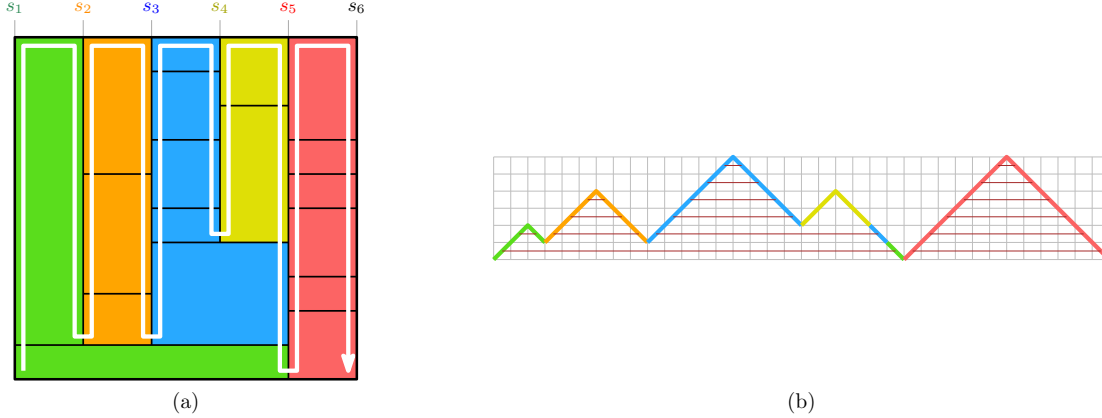(a)   (b)

Fig. 8: A direct bijection between ⊤-avoiding weak rectangulations and Dyck paths. Pairs of vertical sides of the same rectangle in $\mathcal{R}$ correspond to pairs of matching steps in p.

Given a Dyck path p, it is easy to restore the unique rectangulation $\mathcal{R}$ such that $\delta(\mathcal{R}) = p$: one can use the bounding box of p as R, draw a vertical segment upwards from every valley, and then the pairs of matching steps indicate how rectangles should be inserted between the vertical sides and segments of R. This proves that δ is a bijection; therefore τ is also a bijection.   □

The **fourth proof** connects the avoidance of ⊤ to permutation patterns. Let β be the following version of the bijection given by Ackerman, Barequet, and Pinter [1], between weak rectangulations and *Baxter permutations*: Given a weak rectangulation $\mathcal{R}$ of size n, label its rectangles by $1, 2, \ldots, n$ according to the SE–NW ordering, and then read these labels according to the the SW–NE ordering.[iv] The permutation obtained in this way is defined to be $\beta(\mathcal{R})$.

We prove a substantially stronger result which does not just deal with enumeration, but provides a correspondence between a rectangulation pattern and a permutation pattern. Therefore, we give it separately as Theorem 2. It implies $|R^w(\top)| = C_n$ directly, since (213)-avoiding permutations are enumerated by Catalan numbers (and all (213)-avoiding permutations are Baxter).
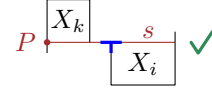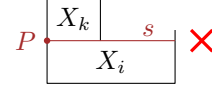
Theorem 2. *A weak rectangulation $\mathcal{R}$ avoids the pattern* ⊤ *if and only the permutation $\pi = \beta(\mathcal{R})$ avoids the pattern* 213.

Proof: Assume that $\mathcal{R}$ contains ⊤, and denote the rectangles adjacent to its joint point by X_i, X_j, X_k as in the drawing. Then, in the SE–NW ordering we have $X_i \prec X_j \prec X_k$, and in the SW–NE ordering we have $X_j \prec X_i \prec X_k$. Hence, π has an occurrence of 213.

$$\frac{X_k}{X_j \mid X_i}$$

Now assume that π contains the pattern 213. Then it necessarily contains $2\underline{13}$ — an occurrence of 213 in which the elements corresponding to 1 and 3 are adjacent. Therefore, $\mathcal{R}$ has three rectangles labeled X_i, X_j, X_k such that we have $X_i \prec X_j \prec X_k$ in the SE–NW ordering, $X_j \prec X_i \prec X_k$ in the SW–NE ordering, and, moreover, X_k is the direct successor of X_i in the SW–NE ordering. Then there is a horizontal segment s that contains the top side of X_i and the bottom side of X_k, and its left endpoint P is the SW-corner of X_k. If X_i extends to the left so that its NW-corner is P, then the left sides of X_i and X_k are contained in the same vertical segment and therefore, a rectangle Y of $\mathcal{R}$ is to the left of X_i if and only if it is to the left of X_k. However, the SE–NW and SW–NE orderings imply that X_j is to the left of X_i but below X_k. Therefore, X_i does not extend to contain P, and hence, the left side of X_i together with s forms ⊤. □

The mappings τ and β are related as the following theorem shows.

Theorem 3. *For every weak rectangulation $\mathcal{R}$ we have $\tau(\mathcal{R}) = \Theta(\beta(\mathcal{R}))$.*

Proof: Let $\pi = \beta(\mathcal{R}) = \pi_1\pi_2\ldots\pi_n$. This means: for every j, the rectangle Y_j labeled j in the SW–NE labeling is labeled π_j in the SE–NW labeling. Therefore, the number of indices i such that $i < j$ and $\pi_i > \pi_j$ is equal to the number of rectangles that occur earlier than Y_j in the SW–NE ordering but later than Y_j in the SE–NW ordering. This is precisely the number of rectangles to the left of Y_j, and therefore, the j-th component of $\Theta(\beta(\mathcal{R}))$ is precisely the L-label of Y_j. Hence, $\Theta(\beta(\mathcal{R}))$ coincides with $\tau(\mathcal{R})$. □

For example, for $\mathcal{R}$ from Figure 7, we have $\beta(\mathcal{R}) = 7\ 18\ 15\ 16\ 17\ 8\ 11\ 12\ 13\ 14\ 9\ 10\ 1\ 2\ 3\ 4\ 5\ 6\ 7$, whose inversion sequence is indeed $e = (0, 0, 1, 1, 1, 4, 4, 4, 4, 4, 8, 8, 12, 12, 12, 12, 12, 12)$, see Figure 9.
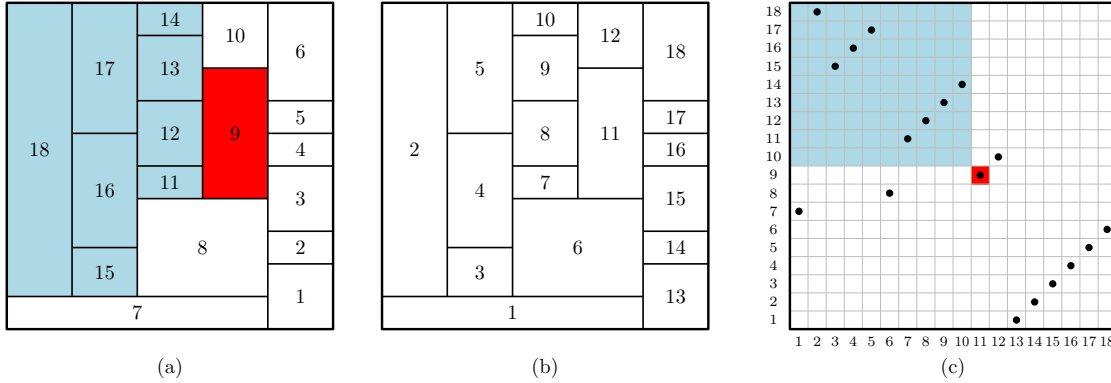

Fig. 9: Illustration to Theorem 3: (a) The SE–NW labeling of $\mathcal{R}$. (b) The SW–NE labeling of $\mathcal{R}$. (c) The permutation $\beta(\mathcal{R})$: $\Theta(\beta(\mathcal{R}))$ coincides with $\tau(\mathcal{R})$. The highlighted areas illustrate $\pi_{11} = 9$ and $e_{11} = 8$.

4.1.2 Classes of inversion sequences enumerated by A279555

Now we turn to the enumeration of ⊤-avoiding *strong* rectangulations. Mütze and Namrata [34] explored them computationally and observed that the first elements of their enumerating sequence match A279555. In the OEIS, A279555 is defined as the enumerating sequence of two classes of inversion sequences, $I(010, 110, 120, 210)$ and $I(010, 100, 120, 210)$. To our knowledge, these classes were first considered by Martinez and Savage in their study of classes of inversion sequences that avoid triples of relations [29]. In their classification, these are classes 764A and 764B; in [29, Theorem 62] they show that these classes are Wilf-equivalent. At the time of writing, these two classes of inversion sequences are the only interpretations of A279555 in OEIS. However, this sequence has been proven, or conjectured, to enumerate some additional classes of inversion sequences, as outlined below.

In [48, Theorem 8.1], Yan and Lin proved that $I(011, 201)$ and $I(011, 210)$ (their classes 3091A and 3091B) are Wilf-equivalent, and conjectured that they are also enumerated by A279555 [48, Conjecture 8.3]. To the best of our knowledge, this conjecture had not been proven at the time of writing. We provide a proof in Theorem 11.

In [20, Section 4.5], Kotsireas, Mansour, Yıldırım constructed a generating tree for $I(011, 201)$ and gave a functional equation satisfied by the generating function. The expression given in [20, Equation 4.16] contained a typo which was fixed by Pantone [36, Section 6.5], who also computed 500 terms for $I(011, 201)$ and for $I(010, 100, 120, 210)$. His computations showed that the enumerating sequences of these classes coincide at least to that extent — thus, providing strong evidence to the conjecture of Yan and Lin.

In [9, Table 1, Case 166], Callan and Mansour listed nine classes of inversion sequences determined by quadruples of patterns of length 3, which are enumerated, or were conjectured to be enumerated, by A279555. The classes $I(010, 110, 120, 210)$ and $I(010, 100, 120, 210)$ from the original definition of A279555 are their classes 166(8) and 166(6). The classes $I(011, 201)$ and $I(011, 210)$ appear in their list as $I(011, 101, 110, 201)$ (class 166(3)) and $I(011, 101, 110, 210)$ (class 166(4)).[v] Thus, Conjecture 1.2 [9] by Callan and Mansour is equivalent to Conjecture 8.3 [48] by Yan and Lin.

From the results achieved in [9, 20, 29, 36, 48] it is known at the time of writing that:

- The classes $166(6-9)$ are Wilf-equivalent and enumerated by A279555,

- The classes $166(1-5)$ are Wilf-equivalent and *conjecturally* enumerated by A279555.

We summarize these results in Table 2, which is adapted from [9, Table 1, Case 166].

In this section we show that $R^s(\top)$ is equinumerous to classes 166(3,6,7,8) from Table 2 by constructing generating trees and also by giving explicit bijections. First, in Section 4.1.3, we show that $R^s(\top)$ is equinumerous to $I(010, 101, 120, 201)$, $I(010, 110, 120, 210)$ and $I(010, 100, 120, 210)$, thus confirming the conjecture by Mütze and Namrata that $R^s(\top)$ is enumerated by A279555. To the best of our knowledge, it is the first interpretation of this sequence using a combinatorial structure other than a class of inversion sequences. Then, in Section 4.1.4, we show that $R^s(\top)$ is equinumerous to $I(011, 201)$. In Section 4.1.5 we combine these results, which completes the proof of the conjecture that all the classes in Table 2 are Wilf-equivalent and enumerated by A279555.

---

[v] To see that $I(011, 201) = I(011, 101, 110, 201)$ and $I(011, 210) = I(011, 101, 110, 210)$, note that avoidance of 011 directly implies avoidance of 101 and of 110. In [9, Theorem 1], a different proof is given.

	Class	Proofs of Wilf-equivalence	Notation in [29, 48]
(1)	$I(010, 100, 110, 201)$		
(2)	$I(010, 100, 110, 210)$	$(3) \sim (4)$: [48].	
(3)	$I(011, 101, 110, 201)$	$(1-5)$: Isomorphic generating trees [9].	$= I(011, 201)$ [48, 3091A]
(4)	$I(011, 101, 110, 210)$	A279555: conjectured [9, 36, 48].	$= I(011, 210)$ [48, 3091B]
(5)	$I(010, 101, 110, 201)$		(shown in [9]).
(6)	$I(010, 100, 120, 210)$	$(6) \sim (8)$: [29].	[29, 764B]
(7)	$I(010, 101, 120, 201)$	$(6-8)$: Isomorphic generating trees [9].	
(8)	$I(010, 110, 120, 210)$	A279555: (6,8) by definition [29].	[29, 764A]
(9)	$I(010, 101, 120, 210)$	A279555: via bijection to (7) [9].	

Tab. 2: Nine classes of inversion sequences avoiding four patterns of length 3, proven or conjectured to be enumerated by A279555 in [9, 29, 36, 48]. (Adapted from [9, Table 1, Case 166].)

4.1.3 ⊤-*avoiding strong rectangulations: bijections with classes of inversion sequences* $I(010, 101, 120, 201)$*,* $I(010, 110, 120, 210)$*, and* $I(010, 100, 120, 210)$

Denote $I^{(6)} := I(010, 100, 120, 210)$, $I^{(7)} := I(010, 101, 120, 201)$, and $I^{(8)} := I(010, 110, 120, 210)$, in accordance to the case number in Table 2. In this section we prove that $R^s(⊤)$ is equinumerous to these three classes. We first prove it by considering a generating tree T1 given by Pantone [36] for $I^{(6)}$, and showing that it can be also regarded as a generating tree for $R^s(⊤)$. Then we describe explicit bijections between $R^s(⊤)$ and these three classes of inversion sequences.

We begin by exploring the structure of $I^{(7)}$, $I^{(8)}$, and $I^{(6)}$. Let $e = (e_1, e_2, \ldots, e_n)$ be an element of any of these classes, and let $(0 =) e_{a_1} < e_{a_2} < \ldots < e_{a_t}$ be its left-to-right maxima. Then, since e avoids 010 and 120, it satisfies the following condition:

- **Condition A**: For every $j = 1, 2, \ldots, t$, we have $a_j \leq k < a_{j+1} \implies e_{a_{j-1}} < e_k \leq e_{a_j}$.
  (For $j = 1$, the condition just says that we have $e_k = 0$ for all k such that $(1 =) a_1 \leq k < a_2$.)

This means that in the plot of e all the elements lie in rectangular areas $[a_j, a_{j+1} - 1] \times [e_{a_{j-1}} + 1, e_{a_j}]$ to which we refer as *active areas*. (By convention, the first active area is $[a_1, a_2] \times \{0\}$, and the last active area is $[a_t, n] \times [e_{a_{t-1}} + 1, e_{a_t}]$.)

Then, the two remaining patterns imply a condition, specific to each of the classes, concerning elements within active areas:

- For $I^{(7)} = I(010, 101, 120, 201)$, **Condition B1**: In every active area, the elements are weakly decreasing.

- For $I^{(8)} = I(010, 110, 120, 210)$, **Condition B2**: In every active area, the elements are weakly increasing, except for the first element e_{a_j}.

- For $I^{(6)} = I(010, 100, 120, 210)$, **Condition B3**: In every active area, the elements whose value is not equal to its first element e_{a_j}, are strictly increasing.

It is easy to see that every sequence that satisfies condition **A** and any of the conditions **B1**, **B2**, **B3**, belongs to the respective class. That is, conditions **A** and **B1** characterize $I^{(7)}$, conditions **A** and **B2** characterize $I^{(8)}$, and conditions **A** and **B3** characterize $I^{(6)}$. In Figure 10 we give three examples to exhibit these characterizations (active areas are highlighted by orange). Note that these characterizations immediately imply $I^{(7)} \sim I^{(8)} \sim I^{(6)}$: an element of $I^{(8)}$ can be obtained from an element of $I^{(7)}$ by vertical reflection of every active area, except for its first column; and an element or $I^{(6)}$ can be obtained from an element of $I^{(8)}$ by the following transformation: if several elements in the j-th active area have the same value smaller than e_{a_j}, then all of them, except for the last one, are replaced by e_{a_j}. These transformations are clearly bijective; in Figure 10 we apply them to obtain $e_1 \mapsto e_2 \mapsto e_3$. We will primarily deal with $I^{(7)}$, since the condition **B1** appears to be the most natural one.
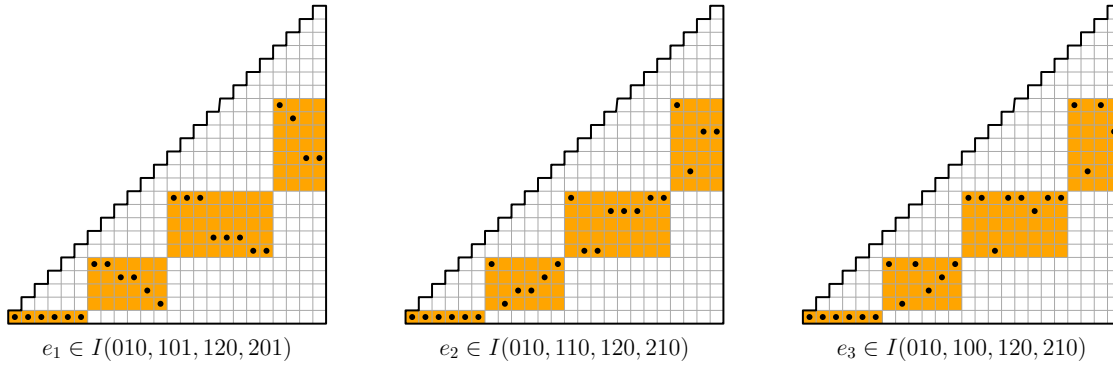

$e_1 \in I(010, 101, 120, 201)$ $e_2 \in I(010, 110, 120, 210)$ $e_3 \in I(010, 100, 120, 210)$

Fig. 10: Examples of inversion sequences in $I^{(7)} = I(010, 101, 120, 201)$, $I^{(8)} = I(010, 110, 120, 210)$, and $I^{(6)} = I(010, 100, 120, 210)$. Active areas are highlighted by orange.

In [36, Section 6.5], Pantone gave the following generating tree[(vi)] T1 for $I^{(6)}$:

Generating Tree T1 [36, Section 6.5]

$$
\begin{aligned}
\text{Root}: \quad & (1, 0). \\
\text{Succession rules}: \quad (k, \ell) \longrightarrow \quad & (1, k-1),\ (2, k-2),\ \ldots,\ (k, 0); & (*) \\
& (k+1, 0),\ (k+1, 1),\ \ldots,\ (k+1, \ell). & (**)
\end{aligned}
$$

Here, k is the bounce[(vii)] of $e \in I_n^{(6)}$, and ℓ is the number of *admissible values* (that is, the values that can be inserted at the end of e to produce a valid element of $I_{n+1}^{(6)}$) which are smaller than M, the maximum of e. The rule $(*)$ represents adding a new maximum (and starting a new active area). The rule $(**)$ represents adding a new value within the last active area of e. We refer to the pair (k, ℓ) for a specific e as the *type* of e.

[(vi)] See, for example, [45] for a brief introduction to the method of generating trees and the related terminology.

[(vii)] Reminder: The bounce of an inversion sequence e is $k = n - M$, where n is the length and M is the maximum value of e.

It is easy to verify that T1 is also a generating tree for $I^{(7)}$ and $I^{(8)}$. In both cases, the statistic k has the same meaning as for $I^{(6)}$ (the bounce). The statistic ℓ for $I^{(8)}$ has the same meaning as for $I^{(6)}$; and the statistic ℓ for $I^{(7)}$ is the number of admissible values which are smaller than the final value of e. (All such values clearly belong to the range of the last active area.) See Figure 11 for the illustration: assuming that a given inversion sequence $e \in I_n^{(7)}$ has the type (k, ℓ), black dots show all admissible values, and the type of $e' \in I_{n+1}^{(7)}$ which is obtained by adding the respective admissible value is shown near every dot.
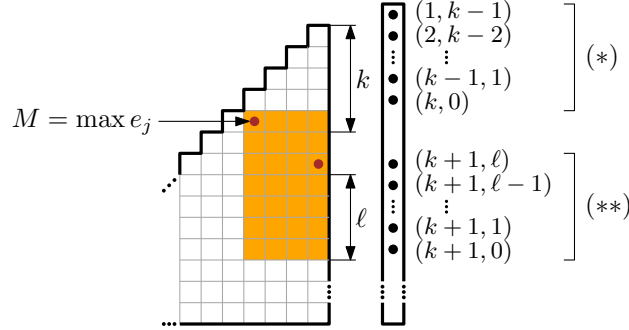

Fig. 11: Illustration for the succession rules of T1 for $I^{(7)}$.

Now we can state and prove the main result of this section.

Theorem 4. *For every $n \geq 1$ we have*

$$|R_n^s(\top)| = |I_n(010, 101, 120, 201)| = |I_n(010, 110, 120, 210)| = |I_n(010, 100, 120, 210)|.$$

Proof: We show that T1 is a generating tree for $R^s(\top)$, where the interpretation of k and ℓ is as follows:

- k is the number of E-rectangles in $\mathcal{R}$,

- ℓ is the number of horizontal segments that neighbor the NE-rectangle of $\mathcal{R}$ on the left.

We refer to the pair (k, ℓ) for a specific $\mathcal{R}$ as the *type* of $\mathcal{R}$. The rectangulation of size 1 has type $(1, 0)$. Given a rectangulation $\mathcal{R} \in R_n^s(\top)$ of type (k, ℓ), we can obtain a rectangulation $\mathcal{R}' \in R_{n+1}^s(\top)$ by inserting a new NE-rectangle in one of the following ways (see Figure 12):

- Inserting a new NE-rectangle while pushing to the left the upper j E-rectangles, where $1 \leq j \leq k$. The new rectangulation has the type $(k - j + 1, j - 1)$. This yields the succession rule $(*)$.

- Inserting a new NE-rectangle while pushing downwards the top edge of the NE-rectangle of $\mathcal{R}$, such that precisely i segments, where $0 \leq i \leq \ell$, touch the new NE-rectangle from the left. The new rectangulation has the type $(k + 1, i)$. This yields the succession rule $(**)$.

These succession rules ensure that every rectangulation in $R^s(\top)$ is generated precisely once: Consider $\mathcal{R}' \in R_{n+1}^s(\top)$, and let X be its NE-rectangle. If the SW-corner of X has the $\perp$ shape or X is an S-rectangle, then $\mathcal{R}'$ is obtained from $\mathcal{R} \in R_n^s(\top)$ by rule $(*)$. If the SW-corner of X has the $\vdash$ shape or
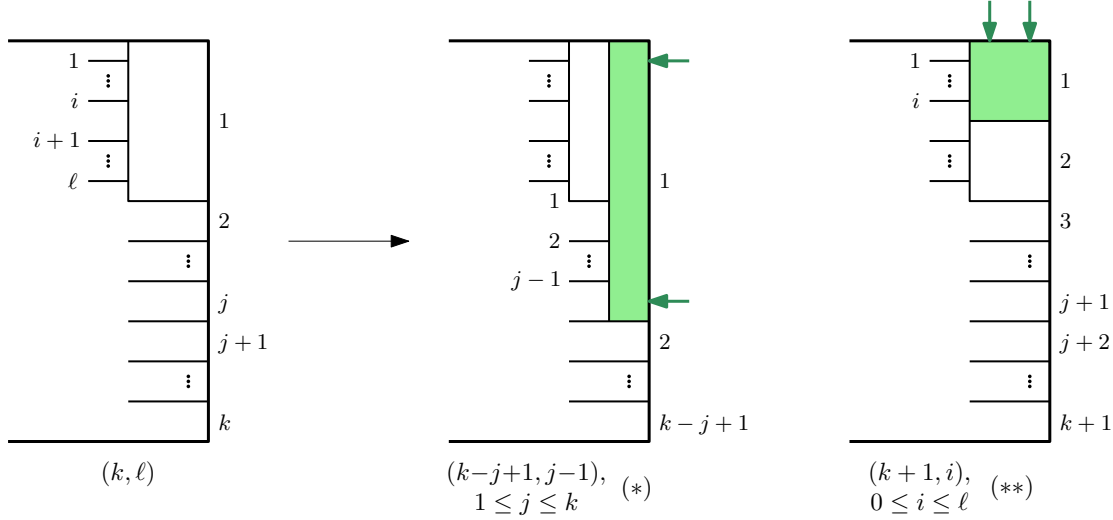
Fig. 12: Illustration for the succession rules of T1 for $R^s(\top)$.

X is a W-rectangle, then $\mathcal{R}'$ is obtained from $\mathcal{R} \in R_n^s(\top)$ by rule $(**)$. In both cases $\mathcal{R}$ obtained from $\mathcal{R}'$ by the (NE) *corner rectangle deletion*, and $\mathcal{R}'$ from $\mathcal{R}$ by the (NE) *corner rectangle insertion* [1, 18]. Thus, we refer to constructing a rectangulation from the size-1 rectangulation by these succession rules as *constructing by* NE *insertion*.

Thus, T1 is a generating tree for $R^s(\top)$. Since it is also a generating tree for $I^{(6)}$, for $I^{(7)}$, and for $I^{(8)}$, the theorem follows.   □

Let $\tau^{(7)} : R^s(\top) \to I^{(7)}$ be the bijection that respects the succession rules of T1 for these two classes, that is: $\tau^{(7)}(\mathcal{R}) = e$ if and only if $\mathcal{R}$ is obtained from the size-1 rectangulation and e is obtained from the size-1 inversion sequence by the same sequence of succession rules. Comparing how the corresponding succession rules of the generating tree T1 act on elements of $I^{(7)}$ and of $R^s(\top)$, it is easy to derive a *direct* description of $\tau^{(7)}$, which modifies the bijection $\tau \colon R^w(\top) \to I(10)$ from the third proof of Theorem 1. Let $\mathcal{R} \in R^s(\top)$, and let $\bar{e} = \tau(\bar{\mathcal{R}})$, where $\bar{\mathcal{R}}$ is the weak rectangulation corresponding to $\mathcal{R}$. Since $\bar{e}$ is non-descending, it belongs to $I^{(7)}$, and its active areas are defined as above. To account for the shufflings along vertical segments in $\mathcal{R}$, we modify $\bar{e}$ as follows: For every k, $2 \leq k \leq t$, consider the neighboring rectangles of the vertical segment s_k, and if the SW-corner of the i-th (bottom to top) right neighbor touches the j-th (bottom to top) left neighbor, we decrease the value of $\bar{e}_{a_k+i-1}$ (the i-th element of the k-th plateau) by $j-1$. Since the jump from the $(k-1)$-th to the k-th plateau of $\bar{e}$ is the number of rectangles that neighbor s_k on the left, the new value is larger than $\bar{e}_{a_k-1}$ — that is, the modified value still belongs to the k-th active area. Finally, it is readily seen that the modified elements of every active area are weakly decreasing.

To visualize this construction, we label, for every s_k, the left neighboring rectangles by $a, b, c, \ldots$ top to bottom, and the right neighboring rectangles by $1, 2, 3, \ldots$ bottom to top, see Figure 13(a). In the plot of $\bar{e}$ we label, for every active area, its rows $a, b, c, \ldots$ from bottom to top, and its columns by $1, 2, 3, \ldots$

from left to right. Then we shift the dots of the plateau so that we have, with respect to this local labeling, the dot (v, w) if and only if the SW-corner of the right neighbor of s_k labeled v lies on the boundary of the left neighbor of s_k labeled w. Then $\tau^{(7)}(\mathcal{R})$ is the inversion sequence e obtained in this way, see Figure 13(b) for an example.
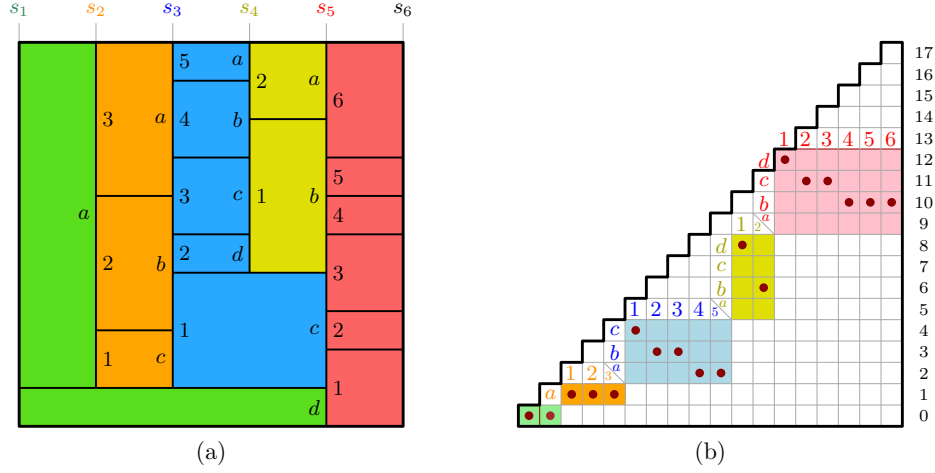

Fig. 13: Illustration to Theorem 4. (a) Rectangulation $\mathcal{R} \in R^s(\top)$. (b) $\tau^{(7)}(\mathcal{R}) \in I(010, 101, 120, 201)$.

For bijections $\tau^{(8)} \colon R^s(\top) \to I^{(8)}$ and $\tau^{(6)} \colon R^s(\top) \to I^{(6)}$ we apply modifications of active areas as shown in Figure 10. The visualization $\tau^{(7)}$ in terms of (v, w) can be adjusted accordingly, we omit the details. Figure 14 shows $\tau^{(8)}(\mathcal{R})$ and $\tau^{(6)}(\mathcal{R})$ for the same rectangulation $\mathcal{R}$ as in Figure 13.
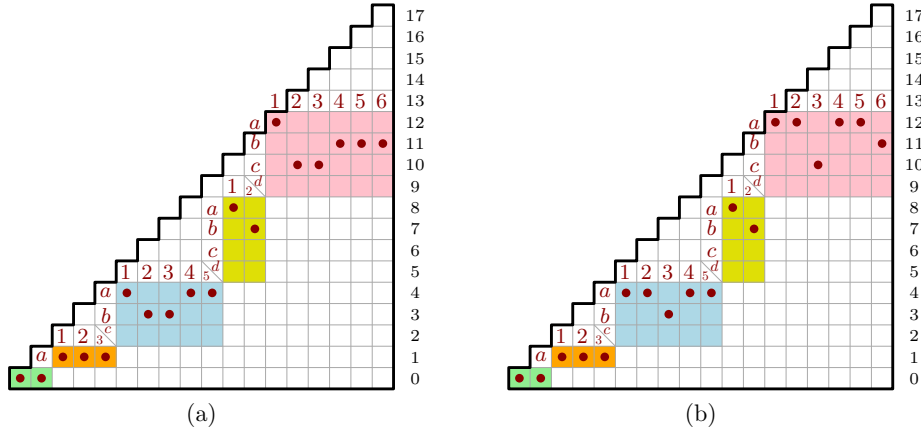

Fig. 14: Illustration to Theorem 4. (a) $\tau^{(8)}(\mathcal{R}) \in I(010, 110, 120, 210)$. (b) $\tau^{(6)}(\mathcal{R}) \in I(010, 100, 120, 210)$.

Finally, we observe which statistics in inversion sequences correspond to the numbers of rectangles that

touch the sides of a rectangulation, under all three bijections $\tau^{(6)}$, $\tau^{(7)}$, $\tau^{(8)}$. These results are directly seen from the explicit description of the bijections, and we omit the proof.

Proposition 5. *Let $\mathcal{R} \in R^s(\top)$, and let e be the image of $\mathcal{R}$ under $\tau^{(6)}$, $\tau^{(7)}$, or $\tau^{(8)}$. Then:*

- *The number of rectangles of $\mathcal{R}$ that touch* N *is the number of left-to-right maxima of e.*

- *The number of rectangles of $\mathcal{R}$ that touch* E *is the bounce of e.*

- *The number of rectangles of $\mathcal{R}$ that touch* S *is the number of high elements in e.*

- *The number of rectangles of $\mathcal{R}$ that touch* W *is the number of 0 elements in e.*

4.1.4 ⊤-*avoiding strong rectangulations: bijection with the class of inversion sequences $I(011, 201)$*

In this section we prove that $R^s(\top)$ is equinumerous to $I(011, 201)$. We use $R^s(\bot)$ instead of $R^s(\top)$, since this leads to a particularly clear visual description. Similarly to the previous section, we first prove the result by considering a generating tree T2 (different from T1) given by Pantone [36] for $I(011, 201)$ and showing that it can be also regarded as a generating tree for $R^s(\bot)$. Then we provide an explicit size-preserving bijection between $R^s(\bot)$ and $I(011, 201)$.

In [36, Section 6.5], Pantone gave the following generating tree T2 for $I(011, 201)$:

Generating Tree T2 [36, Section 6.5]

$$
\begin{aligned}
\text{Root}: &\quad (1, 0). \\
\text{Succession rules}: &\quad (k, \ell) \quad \longrightarrow \quad
\begin{aligned}
&(1, k + \ell - 1),\ (2, k + \ell - 2),\ \ldots,\ (k, \ell); &\quad (*) \\
&(k + 1, 0),\ (k + 1, 1),\ \ldots,\ (k + 1, \ell - 1); &\quad (**) \\
&(k + 1, 0). &\quad (***)
\end{aligned}
\end{aligned}
$$

In this case, k is the bounce of $e \in I_n(011, 201)$, and ℓ is the number of admissible values which are greater than 0 and smaller than M, the maximum value of e. The rule $(*)$ represents adding a new maximum. The rule $(**)$ represents adding an admissible value greater than 0 and smaller than M (since the patterns 011 and 201 are avoided, such a new value is necessarily smaller than the final element of e). The rule $(***)$ represents adding a 0 element. (This explanation is adapted from [36].) See Figure 15 for illustration; white dots represent all the admissible values that can be added to e, and the pairs to the right of corresponding black dots show which type is obtained if this admissible value is added. Note that all the values from $M + 1$ to n are always admissible for $(*)$, and 0 is always admissible for $(***)$. A precise characterization of elements admissible for $(**)$ (denoted by $v_1, v_2, \ldots, v_\ell$ in Figure 15) will be provided in Proposition 7.

Before dealing with rectangulations, we introduce certain geometric relations. If X and Y are two segments, or two rectangles, or one segment and one rectangle, we say that one of them *lies higher than / lies lower than / lies to the left of / lies to the right of* the other if there is a horizontal or vertical line that (weakly) separates them accordingly. (Note that these relations are different from the relations *above*, *below*, etc., used earlier.)

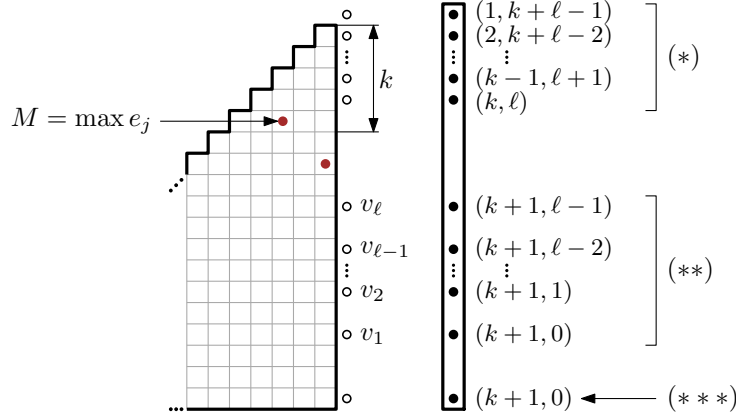**Theorem 6.** *For every $n \geq 1$ we have $|R^s(\bot)| = |I(011, 201)|$.*

Fig. 15: Illustration for the succession rules of T2 for $I(011, 201)$.

Proof: We say that a ⊤ joint is *active* if the right endpoint of its horizontal segment lies on E.
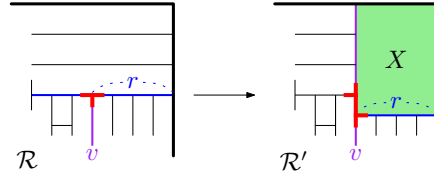
We show that T2 is a generating tree for $R^s(\bot)$, where the interpretation of k and ℓ is as follows:

- k is the number of N-rectangles of $\mathcal{R}$,

- ℓ is the number of active ⊤ joints.

The rectangulation of size 1 has type $(1, 0)$. Given a rectangulation $\mathcal{R} \in R^s_n(\bot)$ of type (k, ℓ), we can obtain a rectangulation $\mathcal{R}' \in R^s_{n+1}(\bot)$ by inserting a new NE-rectangle in one of the following ways (see Figure 16):

- Inserting a new NE-rectangle X while pushing downwards the j right-most N-rectangles, where $1 \le j \le k$, so that all the horizontal segments that exist in $\mathcal{R}$ are lower than the bottom side of X (in particular, X has no left neighboring segments). This decreases the number of N-rectangles by $j-1$ and increases the number of active ⊤ joints by $j-1$; hence, $\mathcal{R}'$ has the type $(k-j+1, \ell+j-1)$. This yields the succession rule $(*)$.

- Inserting a new NE-rectangle X by the following operation: Given an active ⊤ joint, let v be its vertical segment and let r be the right part of its horizontal segment (see the image). Push r slightly downwards so that all the horizontal segments that were lower than r in $\mathcal{R}$ are still lower than the shifted r in $\mathcal{R}'$, shorten accordingly the vertical segments whose upper endpoints lie on r, and extend v upwards to N while truncating from the right the horizontal segments that it meets. The new rectangle X is bounded by N, E, and (modified) r and v. If we perform this operation on the i-th from the right active ⊤ joint, where $1 \le i \le \ell$, this increases k by 1 and sets ℓ to be $i - 1$, since the horizontal segments of active ⊤ joints to the right of the chosen one still reach E, but those of active ⊤ joints to the left of the

chosen one are truncated. Therefore, the new rectangulation $\mathcal{R}'$ has the type $(k + 1, i - 1)$, and we obtain the succession rule $(**)$.

- Inserting a new rectangle that extends from N to S at the right of $\mathcal{R}$. The new rectangulation $\mathcal{R}'$ has the type $(k + 1, 0)$. This yields the succession rule $(***)$.
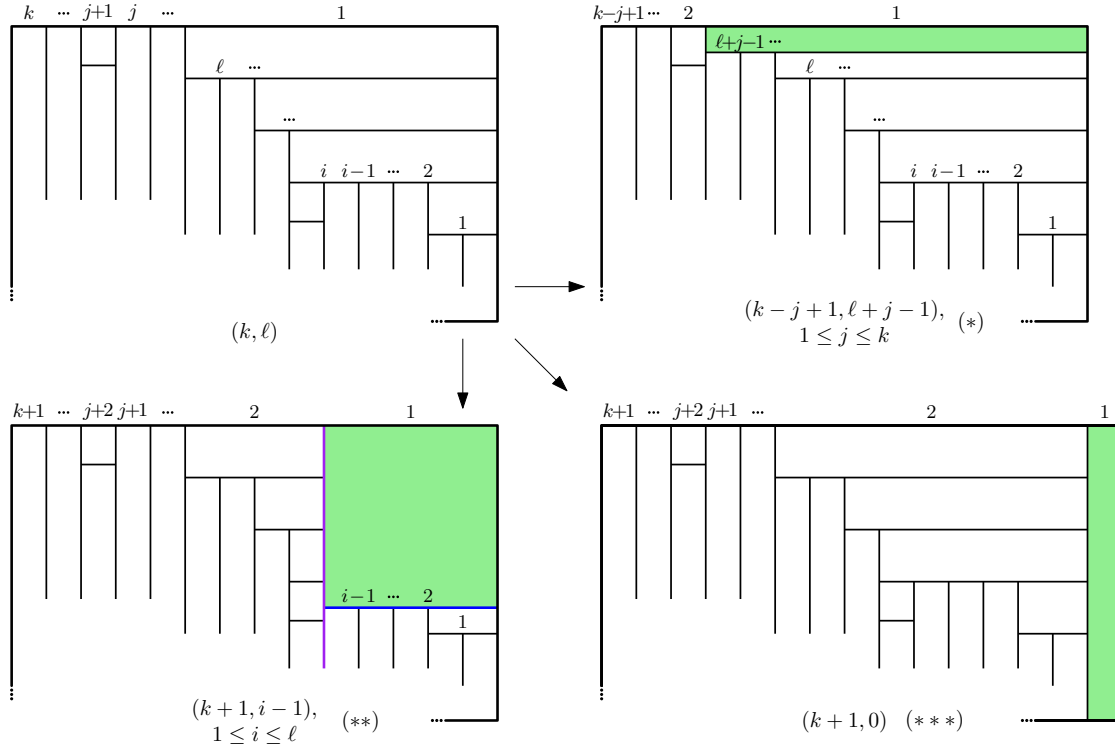

Fig. 16: Illustration for the succession rules of T2 for $R^s(\perp)$.

These succession rules ensure that every rectangulation in $R^s(\perp)$ is generated precisely once. To see that, consider $\mathcal{R}' \in R^s_{n+1}(\perp)$, and let X be its NE-rectangle. Note that the SW-corner of X has the $\vdash$ shape, unless the corner lies on the boundary of R. If X is not an S-rectangle and the left side of X has no neighboring segment on the left, then $\mathcal{R}'$ is obtained from $\mathcal{R} \in R^s_n(\perp)$ by rule $(*)$, whereas $\mathcal{R}$ is the rectangulation obtained from $\mathcal{R}'$ by the corner rectangle deletion. If X is not an S-rectangle and the left side of X has at least one neighboring segment on the left, then $\mathcal{R}'$ is obtained from $\mathcal{R} \in R^s_n(\perp)$ by rule $(**)$. To obtain $\mathcal{R}$ from $\mathcal{R}'$ in this case, we shift the bottom side of X upwards (while respective extending of its bottom neighbors) until it aligns with the lowest left neighboring segment and, thus, a $+$ shape is created; we cut off the portion of the vertical segment from the crossing point upwards; and if there are some horizontal segments whose right endpoints were on the vertical segment which is now cut off, we

extend them to the right so that they touch E. Finally, if X is an S-rectangle then $\mathcal{R}'$ is obtained from $\mathcal{R} \in R_n^s(\bot)$ by rule $(***)$, whereas $\mathcal{R}$ is the rectangulation obtained from $\mathcal{R}'$ by deleting the right-most rectangle. Since at every step of constructing a rectangulation we insert a new NE-rectangle, we refer to it as *constructing by* NE *insertion* (although it is different from the "classical" insertion of a NE-rectangle when $(**)$ is applied).

Thus, T2 is a generating tree for $R^s(\bot)$. Since it is also a generating tree for $I(011, 201)$, the theorem follows. $\qquad\square$

Let $\sigma \colon R^s(\bot) \to I(011, 201)$ be the bijection that respects the succession rules of T2 for these two classes. Next we prove two propositions that eventually lead to an explicit description of σ.

Let $e \in I(011, 201)$, and let M be the maximum value of e. Since 011 is forbidden, all the non-0 admissible values are not values of e. As mentioned above, the values admissible for $(*)$ are precisely the numbers from $M + 1$ to n, and the unique value admissible for $(***)$ is 0. For the values admissible for $(**)$ we know that they are greater than 0 (which is the lowest right-to-left minimum of e) and smaller than e_n (which is the highest right-to-left minimum of e). In order to give an explicit description of σ, we need a more precise information concerning the position of values admissible for $(**)$ between the right-to-left minima of e.

Let $(0 =) e_{b_0} < e_{b_1} < \ldots < e_{b_u}(= e_n)$ be the right-to-left minima of e. Denote by ℓ_i, $1 \leq i \leq u$, the number of values admissible for $(**)$ that lie between $e_{b_{i-1}}$ and e_{b_i}. Then we have $\ell_1 + \ell_2 + \ldots + \ell_u = \ell$, where ℓ is as in the definition of T2. Then we can provide a precise description of the values admissible for $(**)$.

Proposition 7. *For every $1 \leq i \leq u$, the values admissible for $(**)$ that lie between $e_{b_{i-1}}$ and e_{b_i} are precisely $e_{b_i} - \ell_i, e_{b_i} - \ell_i + 1, \ldots, e_{b_i} - 1$. In other words, these are precisely the ℓ_i values just below e_{b_i}. Moreover, $e_{b_i} - \ell_i - 1$ is a value already used in e, and hence, the values admissible for $(**)$ are precisely the values just below e_{b_i}, which are not used in e.*

Proof: As mentioned above, every value admissible for $(**)$ is not used in e, since the pattern 011 is avoided. All we need to prove is that it cannot happen that $e_{b_{i-1}} < a - 1 < a < e_{b_i}$ such that $a - 1$ is admissible and a is not admissible. Assume for contradiction that this happens. If a is a value of e, then we have $a = e_j$ for some $j < b_{i-1}$, since $e_{b_{i-1}}$ and e_{b_i} are two adjacent right-to-left minima. However, in this case $(a)(e_{b_{i-1}})(a - 1)$ is an occurrence of 201, contradicting the assumption that $a - 1$ is admissible. If a is not a value of e, then it forms an occurrence of 201 with some earlier two elements of e. However, in this case $a - 1$ forms an occurrence of 201 with the same two elements.

Similarly, if $e_{b_i} - \ell_i - 1$ not used in e, then, since it is not admissible, it forms an occurrence of 201 with some earlier two elements. However, then $e_{b_i} - \ell_i$ forms an occurrence of 201 with the same two elements. $\qquad\square$

Let $\mathcal{R} \in R_n^s(\bot)$. Label its rectangles by $X_1, X_2, \ldots, X_n$ according to the order in which they were inserted in the NE-insertion.

Proposition 8. *Let $e = \sigma(\mathcal{R}) \in I_n(011, 201)$. Rectangle X_j of $\mathcal{R}$ is an E-rectangle is and only if e_j is a right-to-left minimum of e. Moreover, if we denote such rectangles by $Y_0, Y_1, \ldots, Y_u$, then the number of active ⊤-joints that lie on the bottom side of Y_α is equal to the number of values admissible for $(**)$ just below e_{b_α}.*

Proof: We proceed by induction. Suppose that some succession rule of T2 produces $\mathcal{R}' \in R^s_{n+1}(\bot)$ from $\mathcal{R} \in R^s_n(\bot)$, and $e' \in I_{n+1}(011, 201)$ from $e \in I_n(011, 201)$, and the claim holds for $\mathcal{R}$ and e.

Case 1. If $\mathcal{R}'$ is obtained from $\mathcal{R}$ and e' from e by $(*)$, specifically by $(k, \ell) \to (k - j + 1, \ell + j - 1)$, then $\mathcal{R}'$ has a new E-rectangle X_{n+1}, whose bottom side has $j - 1$ $\top$ joints. On the other hand, e' has a new right-to-left minimum $e_{n+1} = M + j$ which yields $j - 1$ values admissible for $(*)$, namely $M + j - 1, M + j - 2, \dots, M + 1$. There are no changes for existing E-rectangles and their $\top$-joints, and for existing right-to-left minima of e' and values admissible for $(*)$.
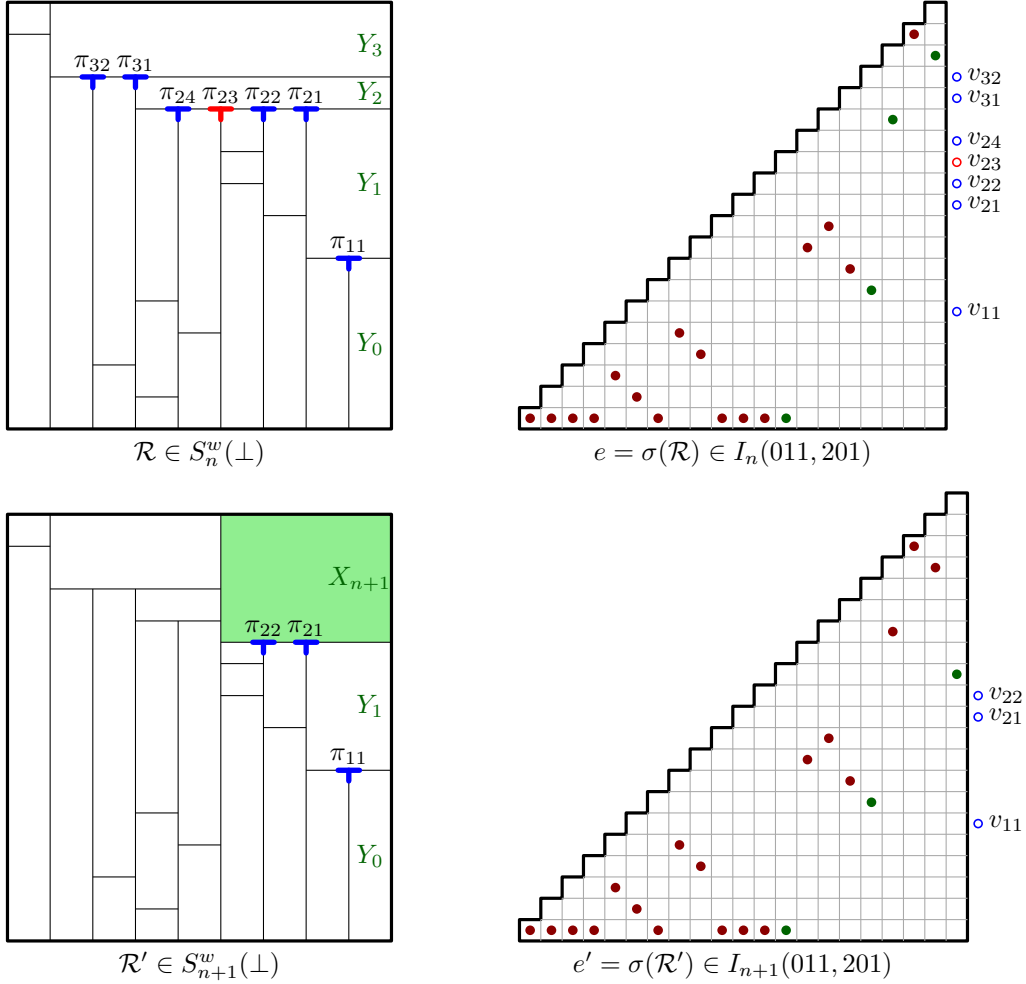

Fig. 17: Illustration to the proof of Proposition 8, Case 2.

Case 2. Suppose $\mathcal{R}'$ is obtained from $\mathcal{R}$ and e' from e by $(**)$. In e, let $v_{\alpha\beta}$ be the β-th, bottom to top, value admissible for $(**)$ between $e_{\alpha-1}$ and e_α, where $\alpha = 1, 2, \dots, u$ and $\beta = 1, \dots, \ell_\alpha$. (In fact we

know from Proposition 7 that $v_{\alpha\beta} = e_{b_\alpha} - 1 - (\ell_\alpha - \beta)$.) In $\mathcal{R}$, let $\pi_{\alpha\beta}$ be the β-th, right to left, active ⊤ joint on the bottom side of Y_α, where $\alpha = 1, 2, \ldots, u$ and $\beta = 1, \ldots, \ell_\alpha$. (These parameters match for $\mathcal{R}$ and e by the assumption.)

The active ⊤ joints are ordered so that $\pi_{\alpha'\beta'}$ lies to the left of $\pi_{\alpha\beta}$ if and only if either $\alpha < \alpha'$ or $\alpha = \alpha'$ and $\beta < \beta'$. From comparing the rule $(**)$ for $I(011, 201)$ and for $R^s(\bot)$ we know that the right-to-left ordering of active ⊤ joints in $\mathcal{R}$ corresponds to the bottom-to-top ordering of the values admissible for $(**)$ in e. Therefore, applying the rule $(**)$ such that $\pi_{\alpha\beta}$ is modified in $\mathcal{R}$ corresponds to adding the admissible value $v_{\alpha\beta}$ in e. Then, in $\mathcal{R}'$, the E-rectangles are $Y_0, Y_1, \ldots, Y_{\alpha-1}, X_{n+1}$, the active ⊤ joints of $Y_1, Y_2, \ldots, Y_{\alpha-1}$ are unchanged, and the active ⊤ joints of X_{n+1} (which assumes the role of Y_α in $\mathcal{R}'$) are $\pi_{\alpha 1}, \pi_{\alpha 2}, \ldots, \pi_{\alpha(\beta-1)}$. And in e' the right-to-left minima are $e_{b_0}, e_{b_1}, \ldots, e_{b_{\alpha-1}}, v_{\alpha\beta}$, the admissible for $(**)$ values just below $e_{b_1}, e_{b_2}, \ldots, e_{b_{\alpha-1}}$ are unchanged, and the admissible for $(**)$ values just below e_α are $v_{\alpha 1}, v_{\alpha 2}, \ldots, v_{\alpha(\beta-1)}$. See Figure 17 for an illustration.

Case 3. Finally, if $\mathcal{R}'$ is obtained from $\mathcal{R}$ and e' from e by $(***)$, then X_{n+1} is a unique E-rectangle, and there are no active ⊤ joints on its bottom side; and $e_{n+1} = 0$ is a unique right-to-left minimum of e, and there are no admissible values below it. $\qquad\square$

Next we define a labeling of the rectangles of $\mathcal{R} \in R^s(\bot)$ which will be used for assigning the values to e in the explicit definition of σ. We begin with a partial order $\prec_P$ on the horizontal segments of $\mathcal{R}$. For distinct horizontal segments s and t, we first set $s \prec t$ if some point of t is directly above some point of s. (This includes the possibility that either of these points is an endpoint of the respective segment.) We define $\prec_P$ as the partial order obtained by taking the transitive closure of $\prec$. See Figure 18(a), where the Hasse diagram of $\prec_P$ is shown by green lines.

Remark: The partial order $\prec_P$ is an instance of *heap of pieces* order, where the horizontal segments are seen as "pieces" with endpoints on fixed vertical rods. The pieces are free to move vertically along the rods, as long as they do not touch each other, also in their endpoints. Then the heap of pieces order determines which of them are forced to be higher than others. See [23, 42] for more information about heaps of pieces.

Next, we consider $\prec_L$, the linear extension of $\prec_P$ determined by the following rule: If s and t are independent in $\prec_P$, then we set $s \prec_L t$ if s lies to the left of t. Equivalently, $\prec_L$ is obtained from $\prec_P$ iteratively by taking (and deleting) the left-most leaf at every step. (From the perspective of planar posets, $\prec_L$ is the *left-most* linear extension of $\prec_P$.) Every strong rectangulation $\mathcal{R}$ can be drawn so that for all such pairs t lies higher than s; such a drawing will be referred to as a *canonical drawing* of $\mathcal{R}$. In the proof of Theorem 6 we specified that when $(*)$ is applied, all the existing horizontal segments of $\mathcal{R}$ are lower than the bottom side of the new NE-rectangle X; and when $(**)$ is applied, all the horizontal segments that were lower than s are lower than the bottom side of X: a rectangulation obtained in this way is always canonical.

Given $\mathcal{R} \in R^s(\bot)$, we consider its canonical drawing, and we label every horizontal segment s by the number of rectangles of $\mathcal{R}$ that lie lower than s. This label will be denoted by $\lambda(s)$. It is clear that t lies higher than s if and only if $\lambda(t) > \lambda(s)$. Additionally, we define the λ-label of every edge of the bottom side of $\mathcal{R}$ to be 0. Note that if t is the direct successor of s in $\prec_L$, then $\lambda(t) - \lambda(s)$ is the number of rectangles whose top edge is included in t. If t is the lowest segment of $\mathcal{R}$, then $\lambda(t)$ is just the number of rectangles whose top edge is included in t.

Finally, we also define λ-labels for rectangles of $\mathcal{R}$. Note that if a rectangle does not touch S, then its lower edge is an entire segment. The λ-label of a rectangle X is defined to be identical to the λ-label of
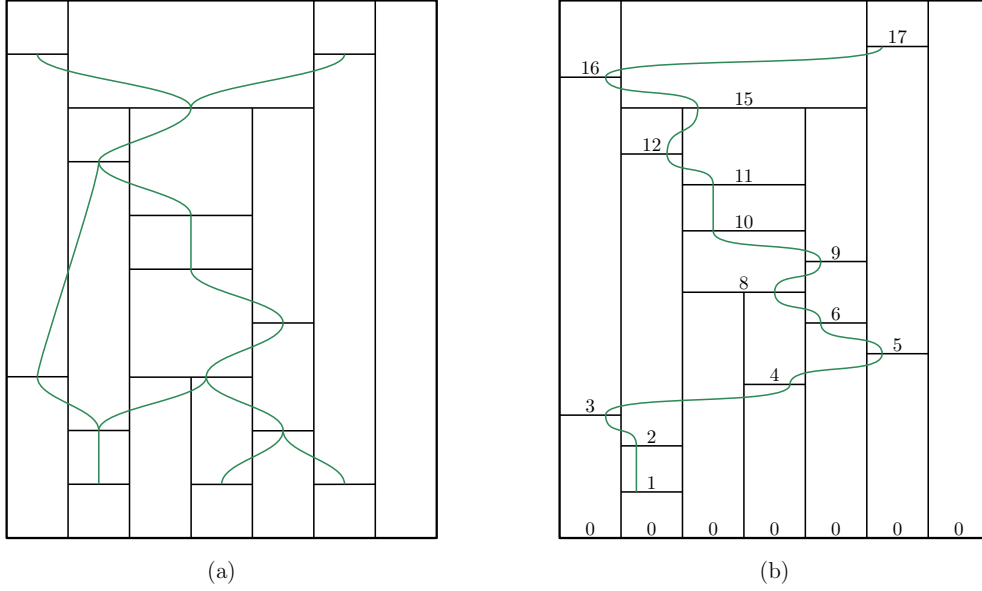
Fig. 18: (a) The partial order $\prec_P$. (b) The linear order $\prec_L$, and the λ-labeling.

its lower edge, and denoted by $\lambda(X)$. In particular, we have $\lambda(X) = 0$ if and only if X is an S-rectangle. See Figure 19(b): every label is the λ-label of the respective rectangle, and also of its lower edge.

Theorem 9. *Let $\mathcal{R} \in R_n^s(\bot)$. Then $e = \sigma(\mathcal{R}) \in I_n(011, 201)$ is obtained by taking the λ-labels of the rectangles of $\mathcal{R}$ in the order of their insertion by the succession rules of T2.*

Proof: We proceed by induction. Assume that $\mathcal{R} \in R_n^s(\bot)$ and $e = \sigma(\mathcal{R}) \in I_n(011, 201)$, $\mathcal{R}' \in R_{n+1}^s(\bot)$ is obtained from $\mathcal{R}$ by one of the succession rules of T2, and $e' \in I_{n+1}(011, 201)$ is obtained by the same succession rule from e. We assume that both $\mathcal{R}$ and $\mathcal{R}'$ are given as canonical drawings.

Suppose that $\mathcal{R}'$ is obtained from $\mathcal{R}$ and e' from e by $(*)$, specifically by $(k, \ell) \to (k - j + 1, \ell + j - 1)$. Then we have $\lambda(X_{n+1}) = (n + 1) - (k - j)$ because the $k - j$ left-most N-rectangles are the only rectangles of $\mathcal{R}'$ which are not lower than X_n. On the other hand, the final value of e is in this case $e_{n+1} = M + j = n + 1 - k + j$. Therefore, the λ-label of the last inserted rectangle is equal to e_{n+1}, and hence, we have $\sigma(\mathcal{R}') = e'$.
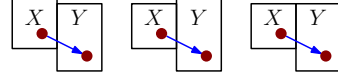
Suppose that $\mathcal{R}'$ is obtained from $\mathcal{R}$, and e' from e by $(**)$, specifically $\mathcal{R}'$ by modifying the $\top$ joint $\pi_{\alpha\beta}$ and e' by adding $e_{n+1} = v_{\alpha\beta} = e_{b_\alpha} - 1 - (\ell_\alpha - \beta)$. Then $\lambda(X_{n+1})$ is equal to e_{n+1}, since in $\mathcal{R}$ the λ-label of the modified horizontal segment was e_{b_α} by induction, and in $\mathcal{R}'$ just $e_{b_\alpha} - (\ell_\alpha + 1 - \beta)$ of these rectangles are lower than X_{n+1}.

Finally, if $\mathcal{R}'$ is obtained from $\mathcal{R}$ and e' from e by $(***)$, then the λ-label of the right-most rectangle is 0, and also $e_{n+1} = 0$. $\square$

To summarize, given $\mathcal{R} \in R^s(\bot)$, we proceed as follows: We consider its canonical drawing and use it to determine the λ-labeling: the λ-labels of the bottom edges are 0, and then we assign the labels going

from bottom to top, and the λ-label of every segment s is the λ-label of the previous segment plus the number of rectangles just below s. To determine the order of taking rectangles, we *delete* NE rectangles and then reverse the order.

There is an even more explicit description of σ. Consider the directed graph T whose nodes are rectangles of $\mathcal{R}$, and there is an edge from X to Y if the SE-corner of X lies on the left side of Y. If there is just one E-rectangle K (in this case we refer to K as the *right-most rectangle*), then T is a (reversed) planar rooted tree with root K. If there is no such K, we augment $\mathcal{R}$ by such a rectangle, which corresponds to adding a 0 value to e.

It is easy to see by considering the succession rules that the last inserted NE-rectangle is always the last node of T (excluding the auxiliary rectangle K) in the *reverse post-order* (that is, for every node, we recursively traverse its subtrees from right to left, and then the node itself).[viii] Hence, we can describe σ as follows: this is an inversion sequence obtained by writing the λ-labels of the rectangles of $\mathcal{R}$, when they are taken in the reverse post-order of T. See Figure 19(a), where the tree T is shown in blue.
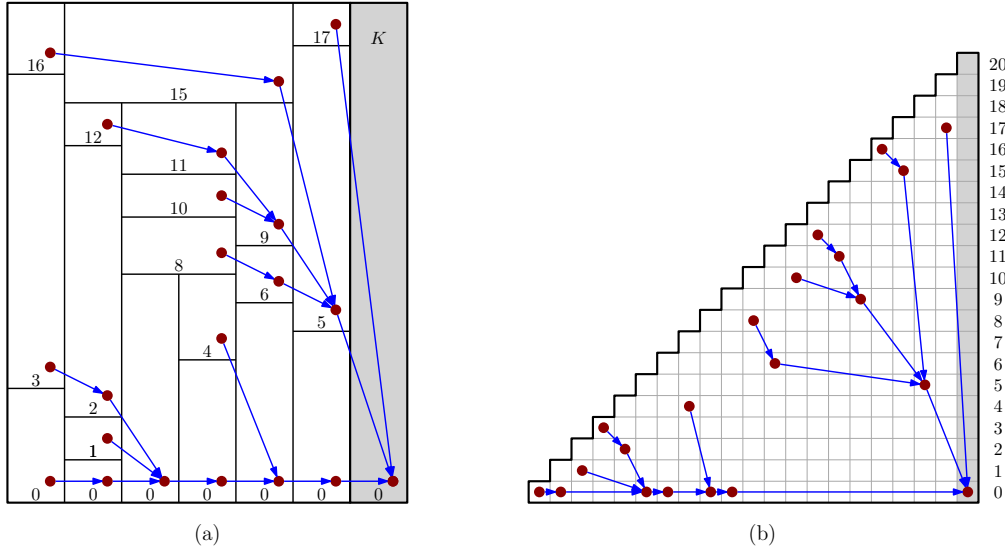

Fig. 19: Illustration to the proof of Theorem 6: (a) A canonical drawing of $\mathcal{R}$ and the tree T (the root K is highlighted by grey). (b) The inversion sequence $f = \sigma(\mathcal{R}) \in I(011, 201)$.

Finally, we can demonstrate the structural identity of $R^s(\perp)$ and $I(011, 201)$ by drawing the corresponding tree over the plot of $e = \sigma(\mathcal{R})$. For two elements e_i and e_j of $e \in I(011, 201)$, we say that (e_i, e_j) is an *inversion* if $i < j$ and $e(j) \leq e(i)$. An inversion (e_i, e_j) is *minimal* if there is no ℓ such

---

[viii] We use the convention that the right-to-left ordering of the subtrees of a node refers to the drawing in which the root is drawn at the top and all the edges are directed upwards. For example, for the rectangle labeled 5 in Figure 19(a), the right-most subtree contains rectangles $8, 6$, the next subtree contains rectangles $10, 12, 11, 9$, and the left-most subtree contains rectangles $16, 15$.

that $i < \ell < j$ and $e(j) \leq e(\ell) < e(i)$. It is easy to see that for every $e_i \neq 0$ except the last element, (assuming that the last value of e is 0) there is a unique j such that (e_i, e_j) is a minimal inversion. Then X_j is a successor of X_i if and only if (e_i, e_j) is an inversion; moreover, X_j is a successor of X_i if and only if (e_i, e_j) is a minimal inversion: both statements are easily seen inductively by following the succession rules. It follows that if we draw the tree over the plot of e where the nodes are the (dots representing the) elements of e and the directed edges connect minimal inversions, then it is isomorphic the to the embedding of T in the drawing of $\mathcal{R}$.

The following statistics of $I(011, 201)$ match the numbers of rectangles that touch the sides of R.

Proposition 10. *Let $\mathcal{R} \in R^s(\perp)$, and let $e = \sigma(\mathcal{R})$. Then:*

(a) *The number of rectangles of $\mathcal{R}$ that touch* N *is the bounce of e.*

(b) *The number of rectangles of $\mathcal{R}$ that touch* E *is the number of right-to-left minima of e.*

(c) *The number of rectangles of $\mathcal{R}$ that touch* S *is the number of 0 elements in e.*

(d) *The number of rectangles of $\mathcal{R}$ that touch* W *is the number of high elements in e.*

Proof: (a) The number of N-rectangles is n minus the λ-label of the highest segment, hence $n - M$. (b) This follows from Proposition 8. (c) A new rectangle is an S-rectangle if and only if the rule $(***)$ is applied. The same rule for e adds 0. (d) A new rectangle is a W-rectangle if and only if the rule $(*)$ with $j = k$ is applied. The same rule adds a high element to e. $\square$

4.1.5   *Summary concerning $I(010, 101, 120, 201)$ and $I(011, 201)$*

Our bijections $\tau^{(7)}$ and σ together provide the proof of the conjecture by Yan and Lin. Moreover, their explicit forms lead to several matching statistics in these classes.

Theorem 11. *For every $n \geq 1$:*

(a) *We have $|I_n(010, 101, 120, 201)| = |I_n(011, 201)|$.*

(b) *The quadruple of statistics (a, b, c, d) for the classes $I_n(010, 101, 120, 201)$, $I_n(010, 110, 120, 210)$, and $I_n(010, 100, 120, 210)$, where*

> a *is the number of 0 elements,*
>
> b *is the number of left-to-right-maxima,*
>
> c *is the bounce,*
>
> d *is the number of high elements.*

matches the quadruple of statistics (x, y, z, t) for the class $I_n(011, 201)$, where

> x *is the number of high elements,*
>
> y *is the number of 0 elements,*
>
> z *is the number of right-left-minima,*
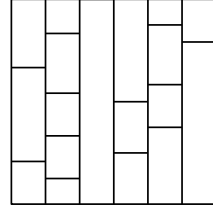>
> t *is the bounce.*

Moreover, a can be switched with c, and x with z.

Proof:

(a) This follows from Theorems 4 and 6 where we proved, by means of bijections $\tau^{(7)}$ and σ, that ⊤-avoiding strong rectangulations are equinumerous to both of these classes of inversion sequences.

(b) This follows from Propositions 5 and 10 (recall that we used ⊤-avoiding rectangulations for $\tau^{(7)}$, and ⊥-avoiding rectangulations for σ). Moreover, due to the horizontal symmetry of these classes (that is, $\mathcal{R}$ belongs to $R^s(\top)$ if and only if the horizontal reflection of $\mathcal{R}$ belongs to $R^s(\top)$) a can be switched with c, and, similarly, x with z. □

4.2 Enumeration and bijections for $R(\top, \bot)$

In this section we consider $(\top, \bot)$-avoiding rectangulations. These are precisely the rectangulations in which every vertical segment reaches N and S. They can be obtained in two steps: The empty rectangle R is first partitioned by vertical cuts into $k \geq 1$ "primary" rectangles $A_1, A_2, \ldots, A_k$, and then every rectangle A_i is further partitioned by horizontal segments into $\ell_i \geq 1$ "secondary" rectangles. We will show that enumeration of $(\top, \bot)$-avoiding weak rectangulations is elementary, but $(\top, \bot)$-avoiding strong rectangulations are bijective to an interesting family of Dyck paths — the so called *rushed Dyck paths*.

4.2.1 $(\top, \bot)$-avoiding weak rectangulations: bijection with compositions

Proposition 12. *For every $n \geq 1$ we have $|R_n^w(\top, \bot)| = 2^{n-1}$.*

Proof: For every n there is a bijection between $(\top, \bot)$-avoiding rectangulations of size n and compositions of n which maps $\mathcal{R}$ to the composition $n = \ell_1 + \ell_2 + \ldots + \ell_k$, where $\ell_1, \ell_2, \ldots, \ell_k$ are as above. For example, the rectangulation in the drawing corresponds to the composition $18 = 3 + 5 + 1 + 3 + 4 + 2$. □

4.2.2 $(\top, \bot)$-avoiding strong rectangulations: bijection with rushed Dyck paths

We use the equivalent set of patterns $\{\vdash, \dashv\}$. We show that $(\vdash, \dashv)$-avoiding strong rectangulations are equinumerous with two families of Dyck paths: *rushed Dyck paths* and *progressive Dyck paths*. A Dyck path is *rushed* if it starts with $h \geq 1$ up-steps and then never visits the altitude h again. A Dyck path is *progressive* if every peak at altitude $h > 1$ is preceded by at least one peak at the altitude $h - 1$.

Both rushed Dyck paths and progressive Dyck paths are enumerated by A287709. In 2018, the first author proved, via telescoping in generating functions, that these families are equinumerous, and Jelínek [19] gave a "semi-bijective" proof based on the involution principle. A direct bijective proof, along with an enumerative formula as well as asymptotic approximations, was recently given by Bacher [6], who also coined the notions of *rushed* and *progressive* Dyck paths. In the following theorem we prove that these kinds of Dyck paths are equinumerious with $(\vdash, \dashv)$-avoiding strong rectangulations.

Theorem 13. *For every $n \geq 1$ and $k \geq 1$, the number of rushed Dyck paths of semilength $n + 1$ and height $k + 1$ is equal to the number of $(\vdash, \dashv)$-avoiding strong rectangulations of size n with $k - 1$ horizontal segments. Therefore, $(\vdash, \dashv)$-avoiding strong rectangulations are enumerated by A287709.*

Proof: Consider the following bijection φ from rushed Dyck paths of semilength ≥ 2 to $R^s(\vdash, \dashv)$, which is adapted from the canonical mapping between Dyck paths and heaps of dimers (see for example [11, Lemma 2] or [43]).

Let P be a rushed Dyck path of semilength $n+1$ that starts with precisely $h = k+1$ up-steps. Consider the usual drawing of P as a lattice path from $(0,0)$ to $(2(n+1), 0)$. Next, consider the grid rectangle $R = [h+1, 2(n+1)] \times [0, h-1]$, and draw horizontal segments along the grid lines to partition R into $h-1$ rectangles on top of each other. For every up-step U of P within R (that is, every up-step of P which is not one of h initial up-steps), draw a vertical segment of height 1 whose midpoint coincides with the midpoint of U. Then $\mathcal{R} := \varphi(P)$ is the rectangle R with horizontal and vertical segments added as described. It has $h-2 = k-1$ horizontal segments and $n+1-h$ vertical segments and hence, it is of size n; and it is clearly $(\vdash, \dashv)$-avoiding. See Figure 20 for an example.
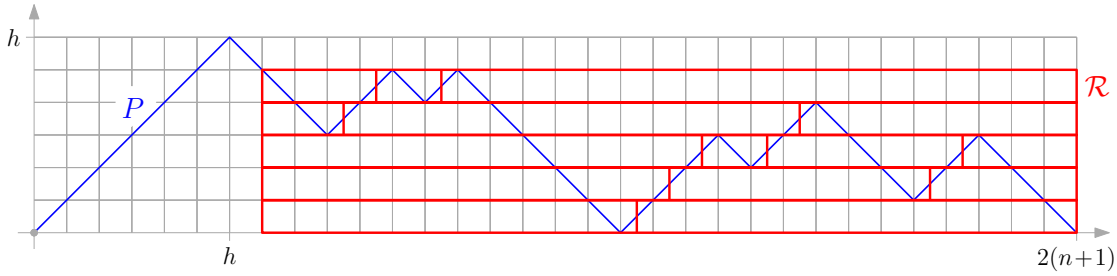

Fig. 20: Illustration for the mapping φ in the proof of Theorem 13: a rushed Dyck path P and the $(\vdash, \dashv)$-avoiding strong rectangulation $\mathcal{R} = \varphi(P)$.

The mapping φ is a bijection, and its inverse φ^{-1} can be described as follows: Given a $(\vdash, \dashv)$-avoiding strong rectangulation $\mathcal{R}$, we first consider the (left-to-right) heap of pieces partial order on the vertical segments of $\mathcal{R}$ (see Figure 21(a)), and then its left-most linear extension (see Figure 21(b)). We draw $\mathcal{R}$ so that its vertical segments occur according to this linear ordering (see Figure 21(b)). Finally, we draw the (unique) Dyck path P such that its baseline contains the bottom side of $\mathcal{R}$, it starts with $k+1$ up-steps, where k is the number of primary rectangles in $\mathcal{R}$, and its non-initial up-steps intersect the vertical segments according to the introduced order. See Figure 21(c) for an illustration.

The path P is clearly a rushed Dyck path. It satisfies $\varphi(P) = \mathcal{R}$ since the order of up-steps in a Dyck path is always the left-most linear extension of their heap of pieces order. It is unique since a Dyck path is uniquely defined by the sequence of the levels of its up-steps. $\square$

The initial up-steps and the first down-step are not essential in a rushed Dyck path. If we delete these steps and flip the path horizontally, we obtain an equivalent family of lattice paths with steps $(1,1)$ and $(1,-1)$ that go from $(0,0)$ to (n,k) and stay (weakly) between the lines $y = 0$ and $y = k$. This is a special case of "Dyck paths in strips". By [22, Example 10.11.2], the generating function for such paths for fixed k is $\dfrac{1}{x\, U_{k+1}\left(\frac{1}{2x}\right)}$, where U_{k+1} is the $(k+1)$-th Chebyshev polynomial of the second kind. Upon the suitable change of variables, we obtain the generating function for $(\vdash, \dashv)$-avoiding strong
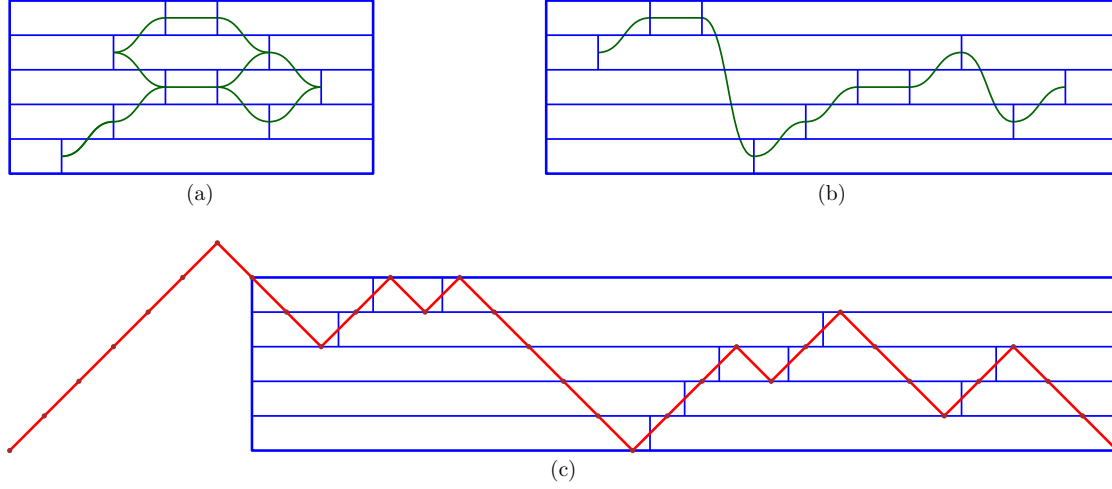
Fig. 21: Illustration for the mapping φ^{-1} in the proof of Theorem 13: (a) A $(\vdash, \dashv)$-avoiding strong rectangulation $\mathcal{R}$ and the heap of pieces poset of its vertical segments; (b) The left-most linear extension of the poset; (c) The rushed Dyck path $P = \varphi^{-1}(\mathcal{R})$.

rectangulations with $k - 1$ horizontal segments:

$$g_k(x) = \frac{x^{\frac{k-1}{2}}}{U_{k+1}\left(\frac{1}{2\sqrt{x}}\right)}.$$

For small values of k, these generating functions are $g_1(x) = \frac{x}{1-x}$, $g_2(x) = \frac{x^2}{1-2x}$, $g_3(x) = \frac{x^3}{1-3x+x^2}$ (A001906, a bisection of the Fibonacci sequence), $g_4(x) = \frac{x^4}{(1-x)(1-3x)}$ (A003462), $g_5(x) = \frac{x^5}{1-5x+6x^2-x^3}$ (A005021), $g_6(x) = \frac{x^6}{(1-2x)(1-4x+2x^2)}$ (A094811), etc. The asymptotic growth rate of the k-th sequence is $4\cos^2(\frac{\pi}{k+2})$.

In the work of Bacher [6, Theorems 4 and 5], similar results are given in terms of Fibonacci polynomials, and also the asymptotics for the number of rushed Dyck path is derived: $\lambda \, 4^n \, e^{-\nu n^{1/3}} \, n^{-5/6} \left(1 + O(n^{-1/3})\right)$, where $\lambda \approx 4.21$ and $\nu \approx 3.18$. Due to our result, this is also the asymptotics for $|R_n^s(\top, \bot)|$.

4.2.3 Restricted classes of permutations and inversion sequences

Here we provide enumerative results for classes of inversion sequences obtained by restricting the bijections from Section 4.1 to $\{\top, \bot\}$-avoiding rectangulations.

$\{\top, \bot\}$-avoiding rectangulations can be characterized as those $\top$-avoiding rectangulations in which every vertical segment is a cut. Accordingly, under τ, $\{\top, \bot\}$-avoiding weak rectangulations correspond to non-decreasing inversion sequences in which all left-to-right maxima are high, or, equivalently, to Dyck paths in which all the valleys are at the x-axis. Hence, restricting the bijection τ from Theorem 1 to

$\{\top, \perp\}$-avoiding rectangulations implies that there are 2^{n-1} such Dyck paths of semilength n — however, this result is, regardless, elementary.

For strong rectangulations, restricting $\tau^{(7)}$ to $R^s(\top, \perp)$ yields the following result:

Proposition 14. $(010, 101, 120, 201)$-*avoiding inversion sequences in which all left-to-right maxima are high, are enumerated by A287709.*

Via $\tau^{(6)}$ and $\tau^{(8)}$ we see that $(010, 110, 120, 210)$-avoiding inversion sequences and $(010, 100, 120, 210)$-avoiding inversion sequences that satisfy the same condition are enumerated by the same sequence.

In context of the bijection σ, $\{\top, \perp\}$-avoiding rectangulations are precisely those in which the number of N-rectangles is equal to the number of S-rectangles. Then Proposition 10(a,c) implies the following result.

Proposition 15. $(011, 201)$-*avoiding inversion sequences e in which the bounce is equal to the number of 0-elements (or, equivalently: in which the set of values is precisely $\{0, 1, \ldots, M\}$, where M is the maximum of e) are enumerated by A287709.*
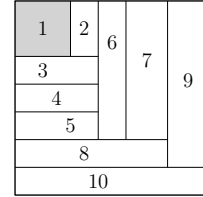
4.3 Elementary models: $R(\top, \vdash)$, $R(\top, \perp, \vdash)$, and $R(\top, \perp, \vdash, \dashv)$

The analysis of the last three classes, $R(\top, \vdash)$, $R(\top, \perp, \vdash)$, and $R(\top, \perp, \vdash, \dashv)$ is elementary to trivial. We include them for the sake of completeness, and also indicate the family of non-decreasing inversion sequences that correspond to these classes under τ.

Proposition 16. $|R_n(\top, \vdash)| = 2^{n-1}$.

Proof. A rectangulation $\mathcal{R}$ is $(\top, \vdash)$-avoiding if and only if every rectangle meets W or N. Indeed, if some rectangle of $\mathcal{R}$ meets neither W or N, then its NW-corner is a part of a $\top$ or a $\vdash$ joint.

Consider the NW–SE labeling of $\mathcal{R} \in R_n(\top, \vdash)$. Then $\mathcal{R}$ is uniquely determined by the binary sequence that indicates which side of R — W or N — the rectangles labeled $2, 3, \ldots, n$ meet. (For example, the rectangulation in the drawing is determined by the sequence NWWWNNWNW.) Hence, there are 2^{n-1} such rectangulations. □
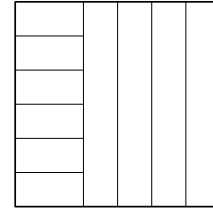

Under the bijection τ from Theorem 1, $(\top, \vdash)$-avoiding rectangulations correspond to non-decreasing inversion sequences in which every jump has height 1.

Observation 17. $|R_n(\top, \perp, \vdash)| = n$.

Proof: A rectangulation in $R_n(\top, \perp, \vdash)$ can be obtained by drawing k vertical segments $(0 \leq k \leq n-1)$ to obtain $k+1$ rectangles, and then adding $n - k - 1$ horizontal segments in the left-most rectangle. Such a rectangulation is uniquely determined by the choice of k, hence $|R_n(\top, \perp, \vdash)| = n$. □

Under the bijection τ, the corresponding inversion sequences have the shape $(0, 0, \ldots, 0, n - k, n - k + 1, \ldots, n - 1)$, where k is the number of vertical segments.

Observation 18. *For $n \geq 2$ we have $|R_n(\top, \perp, \vdash, \dashv)| = 2$.*

Proof: A rectangulation in $R_n(\top, \bot, \vdash, \dashv)$ has either all vertical or all horizontal segments. Thus, there are just two such rectangulations of size n. □

Under the bijection τ, the corresponding inversion sequences are $(0, 0, 0, \ldots, 0)$ and $(0, 1, 2, \ldots, n-1)$.

5   Concluding remarks

This paper is our first report on our study of patterns in rectangulations. In the following parts we thoroughly explore connections between rectangulation patterns and permutation patterns, and provide a catalog of avoidance classes determined by *small patterns* which consist of two or three segments, which leads to interesting phenomena and new surprising links. We hope that this work will serve as a foundation for more general study of pattern avoidance in rectangulations.

Returning to our proof of the conjecture by Yan and Lin, we remark that it is was not least the visual nature of rectangulations that helped us to find the statistics which elucidated a link between two classes of inversion sequences which is somewhat hidden in their structure, and even not easily seen in the plots. This is an additional motivation for the study of rectangulations.

Acknowledgements

References

[1] Eyal Ackerman, Gill Barequet, and Ron Y. Pinter. A bijection between permutations and floorplans, and its applications. *Discrete Appl. Math.*, 154(12):1674–1684, 2006.

[2] Eyal Ackerman, Gill Barequet, and Ron Y. Pinter. On the number of rectangulations of a planar point set. *J. Combin. Theory Ser. A*, 113(6):1072–1091, 2006.

[3] Andrei Asinowski and Cyril Banderier. From geometry to generating functions: Rectangulations and permutations. *Sém. Lothar. Combin.*, 91B:Article 46, 1–12, 2024. Proceedings of the 36th International Conference on Formal Power Series and Algebraic Combinatorics (FPSAC 2024).

[4] Andrei Asinowski, Jean Cardinal, Stefan Felsner, and Éric Fusy. Combinatorics of rectangulations: Old and new bijections. *Combin. Theory*, 5(1):1–57, 2025.

[5] Andrei Asinowski and Toufik Mansour. Separable d-permutations and guillotine partitions. *Ann. Comb.*, 14:17–43, 2010.

[6] Axel Bacher. Progressive and rushed Dyck paths. In Srečko Brlek and Luca Ferrari, editors, *EPTCS, volume 403*, pages 29–34, 2024. Proceedings of the 13th edition of the conference Random Generation of Combinatorial Structures. Polyominoes and Tilings (GASCom 2024).

[7] David Bevan. Permutation patterns: Basic definitions and notation. *arXiv preprint*, arXiv:1506.06673, 2015.

[8] Kevin Buchin, David Eppstein, Maarten Löffler, Martin Nöllenburg, and Rodrigo I. Silveira. Adjacency-preserving spatial treemaps. *J. Comput. Geom.*, 7(1):100–122, 2016.

[9] David Callan and Toufik Mansour. Inversion sequences avoiding quadruple length-3 patterns. *Integers*, 23:Article A78, 1–64, 2023.

[10] Jean Cardinal, Vera Sacristán, and Rodrigo I. Silveira. A note on flips in diagonal rectangulations. *Discrete Math. Theor. Comput. Sci.*, 20(2):Article 14, 1–22, 2018.

[11] Johann Cigler and Christian Krattenthaler. Bounded Dyck paths, bounded alternating sequences, orthogonal polynomials, and reciprocity. *European J. Combin.*, 121:103840, 1–62, 2024.

[12] Sylvie Corteel, Megan A. Martinez, Carla D. Savage, and Michael Weselcouch. Patterns in inversion sequences I. *Discrete Math. Theor. Comput. Sci.*, 18(2):Article 2, 1–21, 2016.

[13] David Eppstein, Elena Mumford, Bettina Speckmann, and Kevin Verbeek. Area-universal and constrained rectangular layouts. *SIAM J. Comput.*, 41(3):537–564, 2012.

[14] Stefan Felsner. Rectangle and square representations of planar graphs. In János Pach, editor, *Thirty essays on geometric graph theory*, pages 213–248. Springer, New York, 2013.

[15] Stefan Felsner, Éric Fusy, Marc Noy, and David Orden. Bijections for Baxter families and related objects. *J. Combin. Theory Ser. A*, 118(3):993–1020, 2011.

[16] Stefan Felsner, Andrew Nathenson, and Csaba D. Tóth. Aspect ratio universal rectangular layouts. *Comput. Geom. Topol.*, 3(1):Article 3, 1–24, 2024.

[17] Ulrich Flemming. Wall representations of rectangular dissections and their use in automated space allocation. *Environment and Planning B: Planning and Design*, 5(2):215–232, 1978.

[18] Xianlong Hong, Gang Huang, Yici Cai, Jiangchun Gu, Sheqin Dong, Chung-Kuan Cheng, and Jun Gu. Corner block list: An effective and efficient topological representation of non-slicing floorplan. In Ellen Sentovich, editor, *Proceedings of the IEEE/ACM International Conference on Computer Aided Design (ICCAD 2000)*, pages 8–12. IEEE Computer Society, 2000.

[19] Vít Jelínek. Personal communication, 2018.

[20] Ilias Kotsireas, Toufik Mansour, and Gökhan Yıldırım. An algorithmic approach based on generating trees for enumerating pattern-avoiding inversion sequences. *J. Symbolic Comput.*, 120:Article 102231, 1–18, 2024.

[21] László Kozma and Thatchaphol Saranurak. Binary search trees and rectangulations. *arXiv preprint*, arXiv:1603.08151, 2016.

[22] Christian Krattenthaler. Lattice path enumeration. In *Handbook of enumerative combinatorics*, Discrete Math. Appl. (Boca Raton), pages 589–678. CRC Press, Boca Raton, FL, 2015. *arXiv preprint:* arXiv:1503.05930 (2015).

[23] Christian Krattenthaler. The theory of heaps and the Cartier–Foata monoid. Appendix in *Commutation and Rearrangements*, an electronic reedition of: Pierre Cartier, Dominique Foata, Problèmes combinatoires de commutation et réarrangements (Lecture Notes in Mathematics, Vol. 85, 1969), Séminaire Lotharingien de Combinatoire / Books, 2006.

[24] Marc van Kreveld and Bettina Speckmann. On rectangular cartograms. *Comput. Geom.*, 37(3):175–187, 2007.

[25] David P. La Potin and Stephen W. Director. Mason: A Global Floorplanning Approach for VLSI Design. *IEEE Trans. Comput. Aided Des. Integr. Circuits Syst.*, 5(4):477–489, 1986.

[26] Shirley Law and Nathan Reading. The Hopf algebra of diagonal rectangulations. *J. Combin. Theory Ser. A*, 119(3):788–824, 2012.

[27] Thomas Lengauer. *Combinatorial Algorithms for Integrated Circuit Layout*. Applicable Theory in Computer Science. Vieweg+Teubner Verlag, Wiesbaden, 1990.

[28] Toufik Mansour and Mark Shattuck. Pattern avoidance in inversion sequences. *Pure Math. Appl. (PU.M.A.)*, 25(2):157–176, 2015.

[29] Megan Martinez and Carla Savage. Patterns in inversion sequences II: Inversion sequences avoiding triples of relations. *J. Integer Seq.*, 21(2):Article 18.2.2, 1–44, 2018.

[30] Emily Meehan. Baxter posets. *Electron. J. Combin.*, 26(3):Article P3.33, 1–24, 2019.

[31] Emily Meehan. The Hopf algebra of generic rectangulations. *arXiv preprint*, arXiv:1903.09874, 2019.

[32] Arturo Merino and Torsten Mütze. Combinatorial generation via permutation languages. III. Rectangulations. *Discrete Comput. Geom.*, 70(1):51–122, 2023.

[33] William J. Mitchell, J. Philip Steadman, and Robin S. Liggett. Synthesis and optimization of small rectangular floor plans. *Environment and Planning B: Planning and Design*, 3(1):37–70, 1976.

[34] Torsten Mütze and Namrata. Personal communication, 2023.

[35] The On-Line Encyclopedia of Integer Sequences. Published electronically at https://oeis.org/.

[36] Jay Pantone. The enumeration of inversion sequences avoiding the patterns 201 and 210. *Enumer. Combin. Appl.*, 4(4):Article S2R25, 1–12, 2024.

[37] Nathan Reading. Generic rectangulations. *Eur. J. Combin.*, 33(4):610–623, 2012.

[38] David Richter. Some notes on generic rectangulations. *Contrib. Discrete Math.*, 17(2):41–66, 2022.

[39] Richard P. Stanley. *Catalan Numbers*. Cambridge University Press, 2015.

[40] John Philip Steadman. *Architectural Morphology: An Introduction to the Geometry of Building Plans*. Pion, 1983.

[41] Benjamin Testart. Completing the enumeration of inversion sequences avoiding one or two patterns of length 3. *arXiv preprint*, arXiv:2407.07701, 2024.

[42] Gérard Xavier Viennot. Heaps of pieces, I: Basic definitions and combinatorial lemmas. In Gilbert Labelle and Pierre Leroux, editors, *Combinatoire énumérative*, volume 1234 of *Lecture Notes in Mathematics*, pages 321–350. Springer Berlin Heidelberg, 1986. Proceedings of Colloque de Combinatoire Enumerative, Montreal, Canada, 1985.

[43] Gérard Xavier Viennot. Lattice Paths and Heaps. Lecture given at the Conference on Lattice Paths, Combinatorics and Interactions, CIRM, Luminy, 2021. Video available at https://viennot.org.

[44] Gérard Xavier Viennot. The Art of Bijective Combinatorics, Part I: An Introduction to Enumerative, Algebraic and Bijective Combinatorics. IMSc, Chennai, 2016. Video available at https://viennot.org.

[45] Julian West. Generating trees and forbidden subsequences. *Discrete Math.*, 157(1-3):363–374, 1996.

[46] Aaron Williams. Personal communication, 2023.

[47] Shmuel Wimer, Israel Koren, and Israel Cederbaum. Floorplans, planar graphs, and layouts. *IEEE Trans. Circuits and Systems*, 35(3):267–278, 1988.

[48] Chunyan Yan and Zhicong Lin. Inversion sequences avoiding pairs of patterns. *Discrete Math. Theor. Comput. Sci.*, 22(1):Article 23, 1–35, 2020.

[49] Bo Yao, Hongyu Chen, Chung-Kuan Cheng, and Ronald L. Graham. Floorplan representations: Complexity and connections. *ACM Trans. Design Autom. Electron. Syst.*, 8(1):55–80, 2003.